Microtubule Stability in Budding Yeast: Characterization and Dosage Suppression of a Benomyl-dependent Tubulin Mutant

Nathan A. Machin, Janet M. Lee, and Georjana Barnes*

Department of Molecular and Cell Biology, University of California, Berkeley, California 94720

To better understand the dynamic regulation of microtubule structures in yeast, we studied a conditional-lethal β-tubulin mutation *tub2–150*. This mutation is unique among the hundreds of tubulin mutations isolated in *Saccharomyces cerevisiae* in that it appears to cause an increase in the stability of microtubules. We report here that this allele is a mutation of threonine 238 to alanine, and that *tub2–150* prevents the spindle from elongating during anaphase, suggesting a nuclear microtubule defect. To identify regulators of microtubule stability and/or anaphase, yeast genes were selected that, when overexpressed, could suppress the *tub2–150* temperature-sensitive phenotype. One of these genes, *JSN1*, encodes a protein of 125 kDa that has limited similarity to a number of proteins of unknown function. Overexpression of the *JSN1* gene in a *TUB2* strain causes that strain to become more sensitive to benomyl, a microtubule-destabilizing drug. Of a representative group of microtubule mutants, only one other mutation, *tub2–404*, could be suppressed by *JSN1* overexpression, showing that *JSN1* is an allele-specific suppressor. As *tub2–404* mutants are also defective for spindle elongation, this provides additional support for a role for *JSN1* during anaphase.

INTRODUCTION

Biochemical analysis of purified tubulins has shown that microtubules exhibit dynamic instability (Mitchison and Kirschner, 1984; Horio and Hotani, 1986; Kristofferson *et al.*, 1986). That is, under steady-state conditions, individual microtubules stochastically switch between phases of slow growth and rapid shrinkage. This behavior is dependent upon the assembly-dependent hydrolysis of tubulin-bound GTP (Hyman *et al.*, 1992).

Microtubules observed in vivo are also seen to exhibit dynamic instability (Salmon *et al.*, 1984; Cassimeris *et al.*, 1988; Sammak and Borisy, 1988; Shelden and Wadsworth, 1990; Baas *et al.*, 1991). However, the dynamic instability of microtubules in vivo is modulated. For example, in tissue culture cells, interphase microtubule arrays are composed of two distinct populations of microtubules (Kirschner and Schulze, 1986; Schulze and Kirschner, 1986; Cassimeris *et al.*, 1988).

Some of the microtubules behave similarly to those observed in vitro, exhibiting dynamic instability, but others are much more stable. Also, during metaphase and anaphase in tissue culture cells, kinetochore-bound microtubules of the mitotic spindle are dynamically unstable, but their assembly and disassembly is regulated at the kinetochore and at the spindle pole (Mitchison and Salmon, 1992).

Perhaps the most dramatic example of regulated microtubule stability is seen at the transition between interphase and mitosis in mitotically active animal cells. During this time the microtubule cytoskeleton is radically reorganized as the extensive cytoplasmic array of more stable microtubules is replaced by the shorter lived microtubules of the mitotic spindle. Comparison of microtubule dynamics in *Xenopus laevis* oocyte extracts arrested in either interphase or mitosis showed that assembly rates were similar, but that the catastrophe frequency, the frequency with which growing microtubules switch to shrinkage, is much higher in mitotic extracts (Belmont *et al.*, 1990).

* Corresponding author.

The importance of dynamic instability to microtubule function, and to the mitotic cell cycle, is illustrated by the observation that mitotically active tissue culture cells cannot complete anaphase when they are treated with anti-microtubule drugs at concentrations that reduce microtubule dynamics without substantially altering net polymer levels (Jordan *et al.*, 1992, 1993; Wendell *et al.*, 1993). As a result of their inhibitory effect on the cell cycle, at least two of these drugs, taxol and vinblastine, are used as chemotherapeutic agents for the treatment of certain cancers. A better understanding of microtubule dynamics may therefore aid in the design of more effective cancer therapies.

The search for nontubulin regulators of microtubule stability has uncovered a number of molecules, including microtubule-binding proteins and tubulin-modifying proteins (reviewed in Hyams and Lloyd, 1994), and, more recently, microtubule-severing proteins (McNally and Vale, 1993; Shiina *et al.*, 1994). The biochemical characterization of these proteins increases our knowledge of mechanisms that control microtubule behavior. However, the roles played by these proteins in vivo, and their spatial and cell-cycle dependent control, remain unclear. Moreover, it is important to employ a variety of approaches to the identification of proteins that modulate microtubule dynamics in vivo so that the full repertoire of regulators is enumerated.

Microtubules in the yeast *Saccharomyces cerevisiae* are essential for nuclear migration, mitosis, meiosis, and karyogamy. Like the microtubules studied in other eukaryotes, budding yeast microtubules are dynamically unstable in vitro (Davis *et al.*, 1993), and are subject to cell-cycle–dependent remodeling. Budding yeast microtubules are amenable to study for several reasons (reviewed in Huffaker *et al.*, 1987; Barnes *et al.*, 1990), primarily because of the powerful genetic techniques that can be used in this organism, and because of the relatively small number of well-defined functions that microtubules perform.

To better understand the regulation of microtubule stability in *S. cerevisiae*, we undertook a genetic analysis of *tub2–150*, a conditional-lethal β-tubulin mutation that causes growth to be dependent on the presence of a microtubule-destabilizing condition. This property of *tub2–150* led to the proposal that the *tub2–150* mutation causes a deleterious increase in the stability of microtubules (Thomas *et al.*, 1985). A *tub2–150* mutant grows either at low temperature, in the presence of the microtubule-destabilizing drug benomyl, or in combination with a secondary, microtubule-destabilizing, mutation (Thomas *et al.*, 1985; Stearns *et al.*, 1990).

We show that the *tub2–150* mutation causes a single amino acid change in yeast β-tubulin that manifests itself as a spindle elongation defect, consistent with it causing an increase in microtubule stability. *JSN1*, a gene encoding a novel protein of 125 kDa, was isolated as a dosage suppressor of *tub2–150*. Overexpression of *JSN1* in a wild-type strain causes an increase in benomyl sensitivity, and can suppress the spindle elongation defect of one other *TUB2* mutant. Thus, *JSN1* may play a role in mitosis, perhaps by affecting the stability of microtubules.

MATERIALS AND METHODS

Media and Strains

Media for yeast growth and sporulation were as described by (Rose *et al.*, 1990), with the exception of benomyl plates, which were as described by Stearns and Botstein (1988). Benomyl was a generous gift of E.I. du Pont de Nemours (Wilmington, DE). The yeast strains used in this study are derivatives of strain S288C and are listed in Table 1. The integration of the *HIS3* gene to mark auxotrophically the *tub2–150* allele was done as described (Wertman *et al.*, 1992) to generate strain DDY600. All temperatures are given in degrees Celsius.

Growth Rates and Immunofluorescence

Growth rates were determined at timed intervals by measuring the absorbance of cultures either at 600 nm using a spectrophotometer or by using a Klett absorbance meter (New York), and by counting cell numbers using a Coulter Counter (Coulter Electronics, Luton, UK) as described (Pringle and Mor, 1975).

Percent viability for each sample was calculated as the ratio of the number of colonies at permissive conditions to the total cell number as determined by Coulter Counter.

The proportions of unbudded, small budded, and large budded cells were based on counts of 400 cells for each sample. Large buds were defined as being half the size or greater than the mother cell.

Nuclear positions were quantified from 200 large budded cells using 2,6-diamidino-phenylindole (DAPI) and fluorescence microscopy.

Microtubule structures were visualized by indirect immunofluorescence microscopy as described below. Nuclear spindle lengths were quantified from 200 large budded cells. The lengths were defined as follows: short spindles were less than the radius of the mother cell, intermediate spindles were between the length of the radius and the length of the diameter of the mother cell, and long spindles were greater than the diameter of the mother cell.

For characterization of vegetatively growing yeast, cells were grown to early log phase (1–2 × 10^6 cells/ml) in SD or YPD medium. Fixation and immunofluorescence procedures were carried out as described by Pringle *et al.* (1991). Monoclonal antibody YOL1/34, recognizing α-tubulin, was used at 1/200 dilution, and anti-Jsn1p (see below) was used at a dilution of 1/100 against strain DDY829. Fluorescein-conjugated anti-heavy and -light chain secondary antisera were obtained from Organon Teknika-Cappel (Malvern, PA). Cells were viewed using a Zeiss Axioscope microscope (Zeiss, Thornwood, NY). Hypersensitized Technical Pan film (Lumicon, Livermore, CA) (Schulze and Kirschner, 1986) was used for all photography.

Fluorescence-activated Cell Sorting (FACS) Analysis

Determination of the DNA content of cells was done using a modified version of the propidium iodine staining technique (Hutter and Eipel, 1978).

Determining Levels of β-Tubulin

TUB2 (DDY78) and *tub2–150* (DBY1366) strains were grown to midlog phase at 25° (DDY78 was grown in YPD and DBY1366 was

Table 1. Yeast strains used in this study

Strain	Genotype[a]	Source
DDY78	*MATα lys2-801am leu2-3,112 ura3-52*	This laboratory
DDY110	*MATa/α ura3-52/ura3-52 leu2-3,112/leu2-3,112 his4-619/+ lys2-801am*	This laboratory
DDY179	*MATα his4-619*	This laboratory
DDY247	*MATa/α ade2-101am/+ his3-Δ200/his3-Δ200 leu2-3,112/leu2-3,112 lys2-801am/+ trp1-1am/ trp1-1am ura3-52/ura3-52*	This laboratory
DDY426	*MATa/α ura3-52/ura3-52 his3-Δ200/his3-Δ200 leu2-3,112/leu2-3,112 lys2-801am/lys2-801am ade2-101am/+*	This laboratory
DBY1366	*MATa ura3-52 tub2-150*	Botstein laboratory
DBY2057	*MATa ura3-52*	Botstein laboratory
DBY2111	*MATα his4-619 tub2-150*	Botstein laboratory
DBY2395	*MATα his3-Δ200 leu2-3,112 lys2-801 ura3-52 tub1::HIS3 tub3::TRP1 +* pRB594 (*LEU2 tub1-501*)	Botstein laboratory
DBY2397	(Same as DBY2395, but with pRB598 (*LEU2 tub1-603*))	Botstein laboratory
DBY2400	(Same as DBY2395, but with pRB605 (*LEU2 tub1-705*))	Botstein laboratory
DBY2402	(Same as DBY2395, but with pRB613 (*LEU2 tub1-713*))	Botstein laboratory
DBY2403	(Same as DBY2395, but with pRB614 (*LEU2 tub1-714*))	Botstein laboratory
DBY2404	(Same as DBY2395, but with pRB616 (*LEU2 tub1-716*))	Botstein laboratory
DBY2406	(Same as DBY2395, but with pRB619 (*LEU2 tub1-719*))	Botstein laboratory
DBY2416	(Same as DBY2395, but with pRB637 (*LEU2 tub1-737*))	Botstein laboratory
DBY2431	(Same as DBY2395, but with pRB664 (*LEU2 tub1-764*))	Botstein laboratory
DBY2304	*MATa ura3-52 lys2-801am his4-539am tub2-402*	Botstein laboratory
DBY2305	(Same as DBY2304, but with *tub2-403*)	Botstein laboratory
DBY2308	(Same as DBY2304, but with *tub2-404*)	Botstein laboratory
DBY2309	(Same as DBY2304, but with *tub2-405*)	Botstein laboratory
DBY3391	*MATa his3-Δ200 leu2-3,112 ura3-52 cin2::LEU2*	Botstein laboratory
DBY3393	*MATa his3-Δ200 leu2-3,112 ura3-52 cin1::HIS3*	Botstein laboratory
DBY3424	*MATa his4-539 ura3-52 cin2-1*	Botstein laboratory
DBY3444	*MATα his3-Δ200 leu2-3,112 ura3-52 cin4::URA3*	Botstein laboratory
DBY5284	*MATα ade2-101am his4-539am ura3-52 cin4-4*	Botstein laboratory
DBY5283	*MATα ura3-52 cin4-4 tub2-150*	Botstein laboratory
DDY600	*MATa his3-Δ200 ura3-52 lys2-801am leu2-3,112 tub2-150::HIS3*	This study
DDY829	DBY 1366 + pJSN1 (2μ *URA3 JSN1*)	This study
DDY832	*MAT a/α ade2-101am/+ his3-Δ200/his3-Δ200 leu2-3,112/leu2-3,112 lys2-801am/lys2-801am ura3-52/ura3-52 jsn1::LEU2/+*	This study[b]
DDY833	*MATα his3-Δ200 leu2-3,112 lys2-801am ura3-52 jsn1::LEU2*	This study[c]
DDY834	*MATa his3-Δ200 leu2-3,112 lys2-801am ura3-52*	This study[c]
DDY835	*MATa ade2-101am his3-Δ200 leu2-3,112 lys2-801am ura3-52 jsn1::LEU2*	This study[c]
DDY836	*MATα ade2-101am his3-Δ200 leu2-3,112 lys2-801am ura3-52*	This study[c]
DDY837	*MATa/α ade2-101am/+ his3-Δ200/his3-Δ200 leu2-3,112/leu2-3,112 lys2-801am/+ trp1-1am ura3-52/ura3-52 ygl023::HIS3/+*	This study[d]
DDY838	*MATa ade2-101am his3-Δ200 leu2-3,112 trp1-1am ura3-52 ygl023::HIS3*	This study[e]
DDY839	*MATα ade2-101am his3-Δ200 leu2-3,112 lys2-801am trp1-1am ura3-52*	This study[e]
DDY840	*MATα his3-Δ200 leu2-3,112 trp1-1am ura3-52*	This study[e]
DDY841	*MATa his3-Δ200 leu2-3,112 lys2-801am trp1-1am ura3-52 ygl023::HIS3*	This study[e]
DDY842	*MATα his3-Δ200 leu2-3,112 lys2-801am ura3-52 tub2-150::HIS3 jsn1::LEU2*	This study
DDY843	*MATa/α ade2-101am/+ his3-Δ200/his3-Δ200 leu2-3,112/leu2-3,112 lys2-801am/lys2-801am trp1-1am/+ ura3-52/ura3-52 jsn1::LEU2/+ ygl023::HIS3/+*	This study

[a] All strains derived from S288C.

[b] Derived by integrative transformation of DDY426 with pJSN1-γ2.

[c] Sporulation product of DDY832.

[d] Derived by integrative transformation of DDY247 with pYGL023-γ.

[e] Sporulation product of DDY837.

grown in YPD + 40 μg/ml benomyl). Each strain was split into two fresh cultures at 34°. One culture contained YPD + 40 μg/ml benomyl, the other contained YPD only. After 2 h (a period long enough for the *tub2-150* mutant's phenotype to manifest itself), cells were collected and total soluble protein was isolated from all four cultures. After determining protein concentrations, equal amounts of protein from each extract were separated on an 8% polyacrylamide gel, and transferred to a nitrocellulose membrane (Ausubel *et al.*, 1989). The membrane was probed with a rabbit anti-β-tubulin primary antibody (#206, diluted 1/3500), and a donkey anti-rabbit secondary antibody conjugated to horseradish peroxidase (diluted 1/4000). β-Tubulin-antibody complexes were visualized using the Amersham ECL kit (Amersham Life Sciences, Arlington Heights, IL). Several different exposures, and a similar experiment using twice as much protein, gave identical results to those shown (our unpublished observation).

Genetic Techniques and Yeast Transformation

Yeast mating, sporulation, and tetrad analysis were performed as described by Rose et al. (1990). Growth on plates was scored by spotting suspensions of cells in water onto plates using a 32-point inoculator. Yeast cells were transformed with DNA by the lithium acetate method of Ito et al. (1983), as modified by Schiestl and Gietz (1989). Transformants were plated onto SD plates supplemented with the appropriate nutrients to select for cells carrying the plasmid. Plasmids were isolated from yeast by shuttling them through bacteria (Strathern and Higgins, 1991).

Bacterial Techniques

Plasmids isolated from yeast were introduced into *Escherichia coli* strain HB101 by electrotransformation (Sambrook et al., 1989; Strathern and Higgins, 1991). Plasmids were recovered from bacteria and purified using CsCl gradients (Sambrook et al., 1989). Purified plasmids were introduced into frozen competent HB101 or DH5αF' cells using a CaCl-based transformation method (Sambrook et al., 1989).

DNA Manipulations

Standard protocols were followed (Ausubel et al., 1989; Sambrook et al., 1989). Restriction endonucleases and other enzymes were obtained from New England Biolabs (Beverly, MA) or from Boehringer Mannheim (Indianapolis, IN) except *Taq* DNA polymerase, which was obtained from Perkin-Elmer/Cetus (Norwalk, CT) or Promega (Madison, WI), and Sequenase DNA polymerase, which was obtained from United States Biochemical (Cleveland, OH).

Selecting Suppressors

Strain DBY1366 (*tub2–150*) was transformed with a 2μ-based yeast genomic library (Carlson and Botstein, 1982), and plated on SD plates at 34°, to select simultaneously for transformation and suppression of the *tub2–150* Ts⁻ phenotype. A small portion of each transformation was plated on SD plates at 20°, to allow the transformation efficiency to be assessed. Of the transformations incubated at 34°, approximately 80,000 cells were transformed to Ura⁺, of which 164 gave rise to colonies. Of these, 16 grew well (compared with a negative control) upon restreaking on SD plates at 34°. Plasmids from these 16 strains were isolated and re-introduced into DBY1366. Eight of these plasmids conferred a strong Ts⁺ phenotype, and so were selected for further study.

Molecular Analysis of JSN1 and YGL023

The eight plasmids that survived multiple rounds of selection were determined to represent three different suppressing activities by restriction and Southern analysis (Ausubel et al., 1989; Sambrook et al., 1989). One of the six plasmids determined to contain the same suppressing activity was named pJSN1. The *JSN1* open reading frame was localized as described in Figure 7. Overlapping fragments from this and nearby regions were subcloned into pBluescript-based vectors (Stratagene, La Jolla, CA) and used for sequence determination via the dideoxy chain terminating method (Sanger et al., 1977). Some DNA sequence was determined using custom-designed DNA oligonucleotides as primers (generously provided by D. Rio). Only one open reading frame was found that satisfied the criteria diagrammed in Figure 7, and it was named *JSN1*.

A deletion of the *JSN1* gene was created using a γ-disruption scheme (Sikorski and Hieter, 1989; see Figure 7). pJSN1-γ2 was constructed by subcloning the 370-bp *XhoI–HindIII* and 1000-bp *SmaI–HindIII JSN1* fragments into pRS305, a *LEU2*-containing plasmid. pJSN1-γ2 was cut with *HindIII*, linearizing the plasmid and exposing the *HindIII* ends of the *JSN1* fragments. Cut plasmid was purified by agarose gel electrophoresis and used to transform strain DDY426 (*leu2-3, 112/leu2-3, 112*). pJSN1-γ2 was constructed such

that its integration would replace all but 42 codons of the 5' end of *JSN1* (the peptide produced by this 42-codon fragment had previously been shown to be incapable of acting as a dosage suppressor of *tub2–150*, and so is predicted to be inert). The 3' end of the disruption lies within the *JSN1* open reading frame (see Figure 7), and does not disrupt any downstream open reading frames. Several Leu⁺ transformants were sporulated and showed 2:2 segregation of Leu⁺:Leu⁻. DNA hybridization using the 0.7-kb *HindIII–HindIII* DNA fragment of *JSN1* as a probe and immuno-blotting using anti-Jsn1p antibodies confirmed that this strain had the *jsn1::LEU2* allele (Ausubel et al., 1989; Figure 9A; and our unpublished observations).

A deletion of the *YGL023* gene was created by designing custom oligonucleotides based on the sequence of the *YGL023* gene (Chen et al., 1991) and using the polymerase chain reaction to create fragments of *YGL023* with restriction enzyme recognition sites propitious for subcloning into the *HIS3*-containing vector pRS303. This construct, pYGL023-γ, was used in a γ-disruption scheme similar to the one described above for pJSN1-γ2. The 5' end of this disruption interrupts the *YGL023* coding sequence at the tenth codon, and the 3' end lies within the *YGL023* open reading frame, and so does not affect downstream open reading frames.

To determine whether *YGL023* could act as a dosage suppressor of *tub2–150*, a 5.6-kb fragment containing *YGL023* was isolated from plasmid pAX-14 (the generous gift of E. Balzi and A. Goffeau) and cloned into pSM217, a 2μ-based *URA3* plasmid provided by C. Chan.

Preparation of Antiserum

To produce anti-Jsn1p antiserum, the 1.3-kb *HindIII–HindIII* fragment that includes the 3' end of *JSN1* was subcloned into the pATH11 vector, creating a fusion between the E. coli *trpE* gene and *JSN1* (Koerner et al., 1991; see Figure 7).

This plasmid was introduced into strain DH5αF'. The trpE-Jsn1p fusion protein was isolated by preparing inclusion bodies as described by Koerner et al. (1991). Protein samples were run on polyacrylamide gels and stained with Coomassie blue.

Bacterially synthesized trpE-Jsn1p fusion protein was excised from preparative sodium dodecyl sulfate-polyacrylamide gels as described by Drubin et al. (1988). Freund's complete adjuvant was used for the first immunization, and Freund's incomplete adjuvant was used for subsequent immunizations (days 21, 42, 62, 83, and 128). Rabbits were immunized with approximately 400 μg and boosted with approximately 250 μg of fusion protein. Antibodies were affinity purified from serum collected on day 187 by first depleting trpE-specific antibodies on a trpE affinity column, and then collecting antibodies specific for the original trpE-Jsn1p fusion protein. Affinity columns were made by coupling the appropriate protein to CNBr-activated Sepharose beads (Pharmacia, LKB Biotechnology) as previously described (Pfeffer et al., 1983). The specificity of anti-Jsn1p antibodies was evaluated. Whole cell extracts (from strains DDY833–836) were run out on 8% sodium dodecyl sulfate-polyacrylamide gels, and immunoblotting was carried out using the ECL kit (Amersham).

RESULTS

Characterization of tub2–150

The *tub2–150* mutation was isolated on the basis of the increased resistance it imparts against the microtubule-depolymerizing drug benomyl (Thomas et al., 1985). Subsequent analysis revealed that this mutation is unique among a large collection of tubulin mutations in that *tub2–150* mutants actually require microtubule-destabilizing conditions for growth (Thomas et al., 1985). Benomyl, cold growth temperatures, and

mutations in the chromosome instability (*CIN*) genes all destabilize microtubules, and all suppress the growth defect of *tub2–150* strains (Thomas *et al.*, 1985; Stearns *et al.*, 1990).

To better understand the basis of the *tub2–150* phenotype, the sequence of the *tub2–150* allele was determined, and compared with wild type. *tub2–150* has a transition that changes the threonine codon ACT to the alanine codon GCT at amino acid position 238. Because threonines are the targets of protein kinases (Pines and Hunter, 1990), two-dimensional gel electrophoresis was used to compare the mobilities of wild-type and *tub2–150* β-tubulin. No differences were evident (our unpublished observations). Thus, the *tub2–150* mutation apparently does not change the phosphorylation state of β-tubulin.

As yeast cells are sensitive to the levels of β-tubulin (Burke *et al.*, 1989; Bollag *et al.*, 1990; Katz *et al.*, 1990; Weinstein and Solomon, 1990), β-tubulin levels were compared in *tub2–150* and wild-type cells, with and without benomyl, as described in MATERIALS AND METHODS. Under no conditions could a difference in the level of β-tubulin be detected between any of these cultures (Figure 1). Thus, *tub2–150* does not cause a detectable difference in the amount of cellular β-tubulin from that present in wild-type cells. We conclude from this that the growth defects and lethality (see below) caused by the *tub2–150* mutation are due to qualitative, rather than quantitative, changes of the tubulin protein.

To elucidate the nature of the defect caused by *tub2–150*, we quantified the phenotype of a *tub2–150* mutant in five ways. First, as shown in Figure 2, the growth rates of *tub2–150* and wild-type strains were compared in liquid culture with and without benomyl. At 34°, wild-type cells are inhibited for growth by 40 μg/ml benomyl, which slows the cell number doubling time from about 1 h to about 2 h (cell number doubling times were calculated from data in Figure 2). *tub2–150*

benomyl:　+　　+　　-　　-

TUB2:　+　　m　　+　　m

Figure 1. β-Tubulin protein levels are not altered by the *tub2–150* mutation or by benomyl. A "+" in the benomyl row indicates that the culture medium contained YPD + 40μg/ml benomyl immediately before being harvested, and a "−" indicates it contained only YPD. In the *TUB2* row, "+" indicates that a *TUB2* strain (DDY78) was used, and "m" indicates that a *tub2–150* strain (DBY1366) was used.

cells grown under permissive conditions (YPD + 100 μg/ml benomyl at 34°), then shifted to medium without benomyl at 34°, grow very poorly, having a cell number doubling time (after several hours) of about 4 h. The cell density of such cultures plateaus at a level more than 10-fold lower than that of *tub2–150* cultures containing benomyl. Examination of Figure 2 reveals that *tub2–150* cells incubated in YPD have a greater optical density per cell than those incubated in YPD + benomyl. This suggests that, although their rate of cell division is slower than that of *tub2–150* cells incubated with benomyl at 34°, *tub2–150* cells incubated without benomyl continue to increase in size. Consistent with this, we have observed that *tub2–150* cells incubated without benomyl and examined microscopically accumulate as large budded cells (see below) and also have a greater cell size, with haploid *tub2–150* cells having sizes similar to those of wild-type diploid cells. When incubated in YPD + 100 μg/ml benomyl at 34°, *tub2–150* cells have a doubling time of about 1.5 h.

As a second evaluation of the *tub2–150* phenotype, to determine whether *tub2–150* causes a defect in any particular phase of the yeast cell cycle, we quantified the morphological distributions of wild-type and *tub2–150* cells incubated at 34° in YPD with or without benomyl (Table 2). Wild-type cells in YPD without benomyl maintained a relatively constant ratio of unbudded to small budded to large budded cells. Cultures of *tub2–150* cells incubated in YPD without benomyl accumulated a larger fraction of large budded cells over time, primarily at the expense of unbudded cells, indicating a defect in mitosis. As noted above, this helps explain our observation that *tub2–150* cells incubated without benomyl at 34° have a greater optical density per cell than either *tub2–150* cells incubated with benomyl or wild-type cells incubated without it.

As a third measure of the *tub2–150* phenotype, to determine which aspect of mitosis is affected by the *tub2–150* mutation, fluorescence microscopy was used to examine *tub2–150* cells incubated at 34° in YPD with or without benomyl. Cells were fixed and treated with DAPI, a DNA binding dye, to visualize nuclei, and were subjected to indirect immunofluorescence to visualize microtubules (Pringle *et al.*, 1991) (Table 3). We classified large budded cells according to the proximity of their nuclei to the bud neck and according to the presence and length of the mitotic spindle. In wild-type cells, as the bud approaches its mature size, the nucleus moves to the mother-bud junction such that nuclear division ends with the mother cell and bud each receiving one daughter nucleus (Byers and Goetsch, 1975; Byers *et al.*, 1978). Examination of DAPI-stained wild-type cells shows that only 4% of large budded cells have nuclei neither in contact with the bud neck nor undergoing division. Twenty percent of large budded *tub2–150* cells incubated at 34°
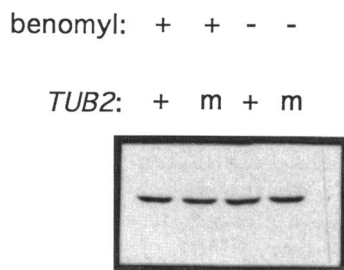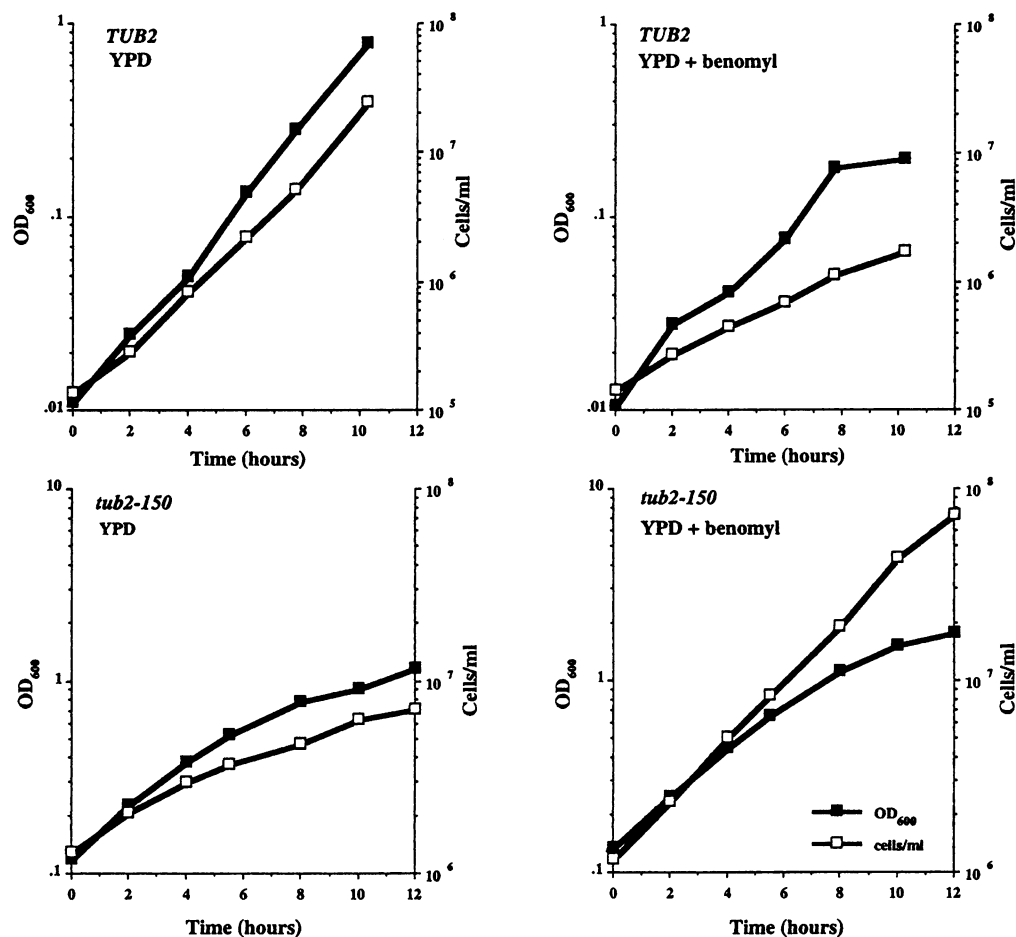
Figure 2. Growth of wild-type and *tub2-150* strains. Optical density and cell number of *TUB2* (DBY2057) and *tub2-150* (DBY1366) strains incubated in YPD and YPD + benomyl were measured. For *TUB2* culture, 40 μg/ml benomyl was used; for *tub2-150* culture, 100 μg/ml benomyl was used.

without benomyl for 4 h have nuclei away from the bud neck. This number is reduced by about one-half in large budded *tub2-150* cells incubated in YPD + 100 μg/ml benomyl at 34°. Nuclear mislocalization is indicative of defects affecting cytoplasmic microtubules (Palmer *et al.*, 1992; Eshel *et al.*, 1993).

Examination of spindle microtubules using immunofluorescence reveals that incubation of *tub2-150* cells in YPD without benomyl leads to a significant increase in the percentage of cells that have short mitotic spindles, relative to *tub2-150* cells incubated in YPD + 100 μg/ml benomyl (Table 3). This increase is accompanied by a reciprocal decrease in the percentage of cells that have longer spindles, suggesting that the *tub2-150* mutation impairs spindle elongation. Incidentally, we noted that many of the short spindles found in mislocalized nuclei are also misoriented; that is, instead of being in line with the mother-bud axis, they are perpendicular to it (see Figure 3). In many of these cells, cytoplasmic microtubules from both spindle pole bodies extend into the bud which, together with the spindle, form a triangular array of microtubules. Such triangles are never seen in wild-type cells

(our unpublished observations). Thus, our quantitative analysis indicates that the *tub2-150* mutation primarily affects nuclear (spindle) microtubule function, but also affects cytoplasmic microtubules.

As a fourth way of characterizing the effect of the *tub2-150* mutation, the viability of *tub2-150* cells incubated in YPD with and without benomyl at 34° was determined (Figure 4). When provided with 100 μg/ml benomyl, *tub2-150* cells retain a viability that approaches 100%. The viability of *tub2-150* cells incubated without benomyl steadily decreases to about 50% after 8 h at 34°. This mimics the effect of benomyl on wild-type cells. Perturbations of microtubule structure in budding yeast lead to a checkpoint-dependent delay in mitosis followed by cell death (Hoyt *et al.*, 1991; Li and Murray, 1991).

Finally, to determine whether *tub2-150* really has a defect in mitosis, as opposed to a defect in S phase, we used FACS analysis (Figure 5) to determine the DNA content of wild-type and *tub2-150* cells. Figure 5A shows that an exponentially growing culture of wild-type cells contains approximately equal numbers of cells with 1N and 2N amounts of DNA. However, a

Table 2. Distributions of cell morphologies of *TUB2* and *tub2-150* cells, with and without benomyl, at 34°

Time[a]	Cell morphology		
	Unbudded	Sm. Budded	Lg. Budded
TUB2 YPD			
0'	51%	20%	30%
30	67	7	26
120	49	20	31
240	42	19	39
360	54	20	27
TUB2 YPD + benomyl[b]			
0	61	12	27
30	68	8	24
120	38	23	40
240	25	11	64
360	27	14	59
tub2-150 YPD			
0	39	17	44
60	38	26	36
120	15	13	72
240	21	16	64
330	19	16	65
tub2-150 YPD + benomyl[b]			
0	42	20	37
60	47	21	32
120	33	18	50
240	38	21	42
330	34	20	47

For each time point, 200 cells were examined. Percentages were rounded to the nearest whole number.

[a] Time after shift from growth in YPD at 34° (for *TUB2* cells) or YPD + 100 μg/ml benomyl at 34° (for *tub2-150* cells) into the indicated medium, at 34°.

[b] 40 μg/ml in YPD for *TUB2*, 100 μg/ml in YPD for *tub2-150*.

haploid *tub2-150* strain grown under permissive conditions and then switched to YPD without benomyl for about one generation accumulates >2N DNA content (Figure 5B). Thus, DNA synthesis is not perturbed, but mitosis is.

A spindle elongation defect such as that caused by *tub2-150* is consistent with a defective interaction between spindle motor proteins and the spindle (Meluh and Rose, 1990; Hoyt *et al.*, 1992, 1993; Roof *et al.*, 1992; Saunders and Hoyt, 1992; Endow *et al.*, 1994). However, the suppression of the *tub2-150* growth defect by microtubule-depolymerizing conditions, and the observation in tissue culture cells that the dynamic instability of microtubules is required for the completion of mitosis (Saxton and McIntosh, 1987; Amin-Hanjani and Wadsworth, 1991; Mitchison and Salmon, 1992; Jordan *et al.*, 1993), suggests that the *tub2-150* mutation causes an increase in the stability of microtubules. Thus, *tub2-150* offers a unique opportunity to examine the regulation of microtubule stability in budding yeast.

Isolation of Dosage Suppressors of *tub2-150*

To find nontubulin determinants of microtubule stability, dosage suppressors of the *tub2-150* phenotype were isolated.

A *tub2-150* mutant strain was transformed with a 2μ-based yeast genomic library, and plated under conditions that selected simultaneously for presence of the plasmid (using the *URA3* gene) and suppression of *tub2-150* (see MATERIALS AND METHODS). The two selections were imposed simultaneously, rather than sequentially, to allow recovery of any suppressors that might be lethal to a *tub2-150* strain grown under its permissive conditions (e.g., by dramatically destabilizing microtubules). From an estimated 80,000 transformants, representing approximately 64 genome equivalents of the library, 164 colonies were recovered. Several rounds of retesting revealed that eight of these contained plasmids that are capable of reproducibly suppressing *tub2-150*. Subsequent molecular analysis revealed that six of these plasmids, although independently isolated, contain identical or overlapping genomic fragments, and therefore are likely to carry the same suppressing activity. Each of the other two suppressing plasmids contain unique genomic fragments, for a total of three suppressing activities. Because these suppressors were selected for their ability to suppress the temperature-sensitive drug dependence, or drug "addiction," of a *tub2-150* strain, we named them the "Just Say No" (*JSN*) suppressors. The suppressor isolated multiple times independently was named *JSN1*, and was the first to be chosen for further study.
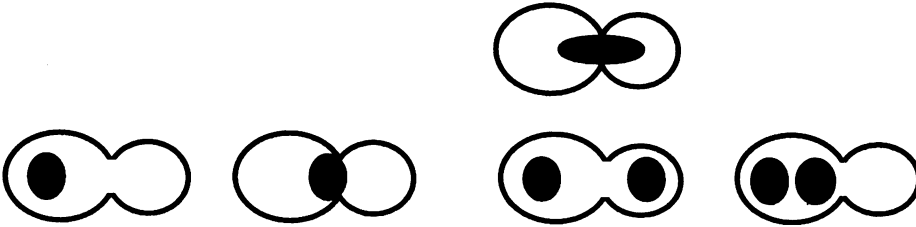
Genetic Characterization of *JSN1*

Figure 6 shows the suppression of *tub2-150* by overexpression of *JSN1*. In the absence of *JSN1* overexpression, and in the absence of benomyl, a *tub2-150* strain grows at 20°, but not 34°. With the *JSN1* overexpressing plasmid (pJSN1), however, the same strain grows well at either temperature.

This effect of *JSN1* overexpression on a mutant presumed to have increased microtubule stability suggests that the *JSN1* gene product might act, directly or indirectly, to destabilize microtubules. This hypothesis was tested by overexpressing *JSN1* in a variety of genetic backgrounds.

Overexpression of *JSN1* in an otherwise wild-type strain leads to increased benomyl sensitivity (Figure 6). This result suggests that the *JSN1* gene product can decrease microtubule stability. It should be noted that the sensitivity of wild-type yeast strains to benomyl is greater at lower temperatures. At all temperatures tested (20°, 25°, 30°, 34°, and 37°), an increase in benomyl sensitivity was observed for strains overexpressing *JSN1*.

Table 3. Distributions of nuclear and spindle microtubule phenotypes in large budded *TUB2* and *tub2-150* cells, with and without benomyl, at 34°

Nuclear phenotypes

Time[a]	Benomyl[b]	Away from neck	At neck	Dividing/divided	Binucleate
tub2-150					
0′	−	14%	74%	13%	2%
120	−	9	73	18	1
240	−	20	60	20	1
0	+	15	71	13	0
120	+	7	64	28	2
240	+	8	67	25	1
TUB2					
120	−	4	56	40	1
120	+	10	82	6	3

Spindle microtubule phenotypes

Time[a]	Benomyl[b]	Dot	Short spindle[c]	Medium spindle[d]	Long spindle[e]
tub2-150					
0′	−	0%	84%	7%	10%
120	−	0	94	5	2
240	−	0	92	7	1
0	+	0	74	18	9
120	+	0	63	21	17
240	+	0	66	16	18
TUB2					
120	−	0	16	24	60
120	+	85	4	7	6

For each time point, 200 large budded cells were examined. Percentages were rounded to the nearest whole number.

[a] Time after shift from growth in YPD at 34° (for *TUB2* cells) or YPD + 100 μg/ml benomyl (for *tub2-150* cells) into the indicated medium, at 34°.

[b] 40 μg/ml in YPD for *TUB2*, 100 μg/ml in YPD for *tub2-150*.

[c] Defined as being less than half a cell diameter in length.

[d] Defined as being between one-half and one cell diameter in length.

[e] Defined as being greater than one cell diameter in length.

As previously mentioned, a large number of tubulin and tubulin-affecting mutations has been isolated in *S. cerevisiae*. The effects of *JSN1* overexpression on the temperature and benomyl sensitivities of a representative set of these mutants were determined (Table 4).

Nine alleles of *TUB1*, four alleles of *TUB2*, and alleles of three *CIN* genes were used. This group of mutants has a variety of phenotypes, including heat- and cold-sensitive growth and altered benomyl sensitivities, and is a representative subset of mutations affecting microtubules.
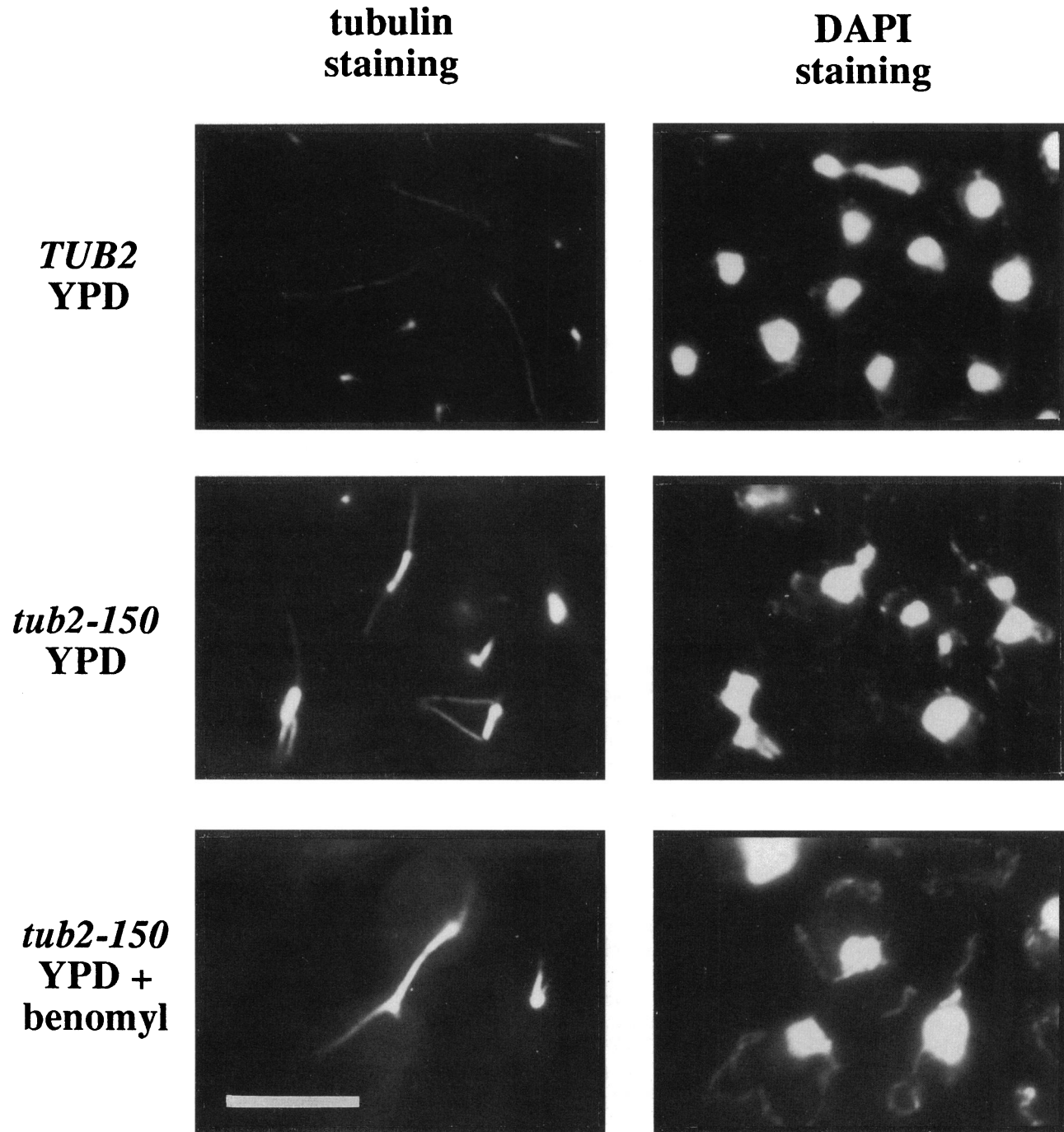
tubulin
staining

DAPI
staining

**TUB2
YPD**

**tub2-150
YPD**

**tub2-150
YPD +
benomyl**

Figure 3. Microtubules in *TUB2* and *tub2–150* cells. Microtubules (left column) and nuclei (right column) were visualized using anti-α–tubulin and DAPI, respectively. *TUB2* cells (strain DDY78) were grown to mid-log phase before being processed. *tub2–150* cells (strain DBY1366) were grown to midlog phase in YPD + 40 μg/ml benomyl at 25°. In the middle row, *tub2–150* cells were then shifted to YPD without benomyl at 34° for 2 h before processing. In the bottom row, *tub2–150* cells were shifted to YPD + 40μg/ml benomyl at 34° for 2 h before processing. Bar, 10 μm.

For most of the mutants, under most of the conditions tested, overexpressing *JSN1* either has no detectable effect or leads to only a small increase in benomyl sensitivity, reminiscent of the results obtained with a wild-type strain. There was one significant exception (Table 4).
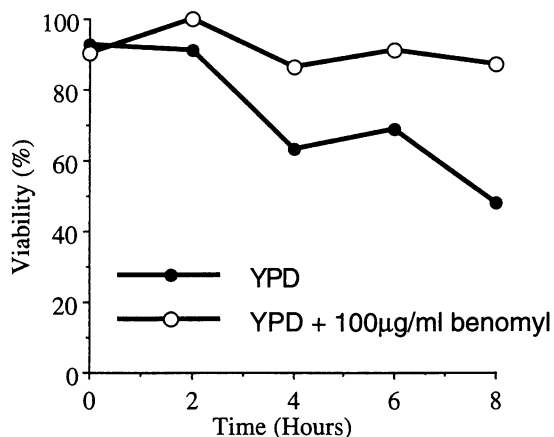
Figure 4. Viability of *tub2–150* mutant with and without benomyl. A *tub2–150* mutant (strain DBY1366) was grown to midlog phase at 34° in YPD + 100 μg/ml benomyl, then shifted to either YPD + 100 μg/ml benomyl or YPD without benomyl at 34° (time 0). The viability of each culture was then determined at timed intervals.

Figure 5. FACS analysis of *TUB2* and *tub2–150* strains. DNA contents of (A) *TUB2* cells (strain DDY179) and (B) *tub2–150* cells (strain DBY1366) were determined, as described in MATERIALS AND METHODS.

The *tub2–404* mutation causes cold-sensitive growth, but wild-type sensitivity to benomyl (Huffaker *et al.*, 1988). When examined using immunofluorescence microscopy, *tub2–404* mutants incubated at nonpermissive temperature are seen, like *tub2–150* mutants, to arrest with a short mitotic spindle (Huffaker *et al.*, 1988). Overexpression of *JSN1* in *tub2–404* at that mutant's permissive temperatures increases its benomyl sensitivity, similar to the effect of *JSN1* overexpression in a wild-type strain. However, *JSN1* overexpression suppresses this mutant's cold sensitivity, allowing it to grow at 14° (see Figure 6).

Molecular Analysis of JSN1

To gain a better insight into how *JSN1* might function, a molecular analysis of this gene was undertaken. Restriction maps of the six isolates of *JSN1* recovered by the selection were constructed. It was found that all six have in common a 5.5-kb region. After showing this region to be sufficient for suppression of *tub2–150*, we generated a restriction map of the fragment, as shown in Figure 7. We used this information to identify smaller fragments capable of suppressing *tub2–150* when overexpressed. As shown in Figure 7, the left-hand limit of the suppressing activity lies between the *Sph*I site and the middle-left *Hin*dIII site. The right-hand limit of the suppressing activity lies between the *Nco*I site and the middle-right *Hin*dIII site. The bar below the restriction map represents this schematically; the suppressing activity extends from one stippled area, through the black region, into the other stippled area. White areas are not required for suppression.
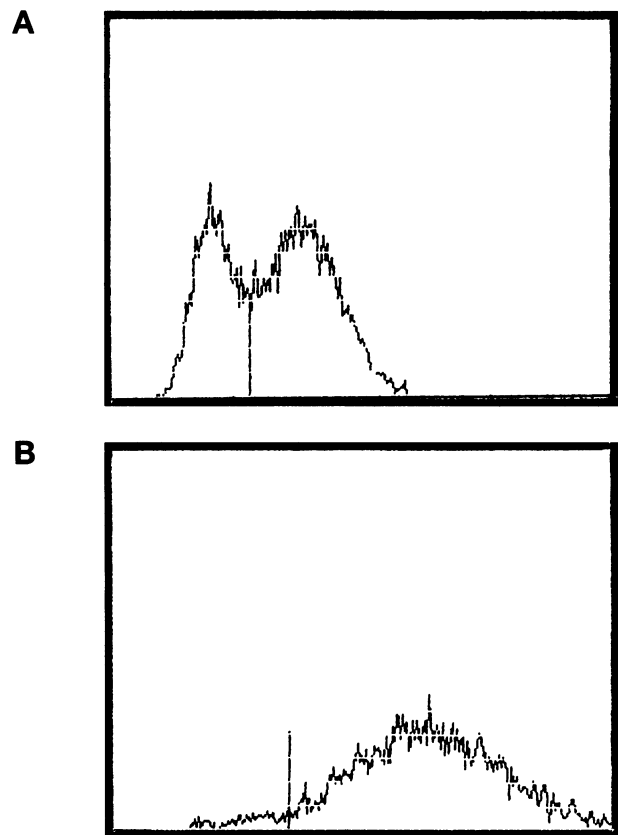
The 0.7-kb *Hin*dIII fragment from this region was used to probe an ordered set of yeast genomic fragments (Olson *et al.*, 1986). This combined with our sequence data (see below) revealed that *JSN1* lies on the right arm of chromosome X, just upstream of a recently identified ORF (GenBank accession number T38151) and *GRR1* (Flick and Johnston, 1991) (Figure 7).

A 3.8-kb segment of DNA from this region was sequenced. Within this region is an open reading frame of 3273 nucleotides, predicted to encode a protein of 1091 amino acids (Figure 8A). It is the only open reading frame spanning across the left-middle *Hin*dIII site and the *Nco*I site (see Figure 7), and therefore corresponds to the *JSN1* open reading frame. Note that the 3' end of *JSN1* extends beyond the middle-right *Hin*dIII site, and so is dispensable for suppression of *tub2–150*.

The GenBank protein sequence library was searched for sequences identical or similar to the predicted sequence of Jsn1p. No exact matches were found, indicating that Jsn1p is a previously unidentified protein. Throughout most of its length, Jsn1p is a unique
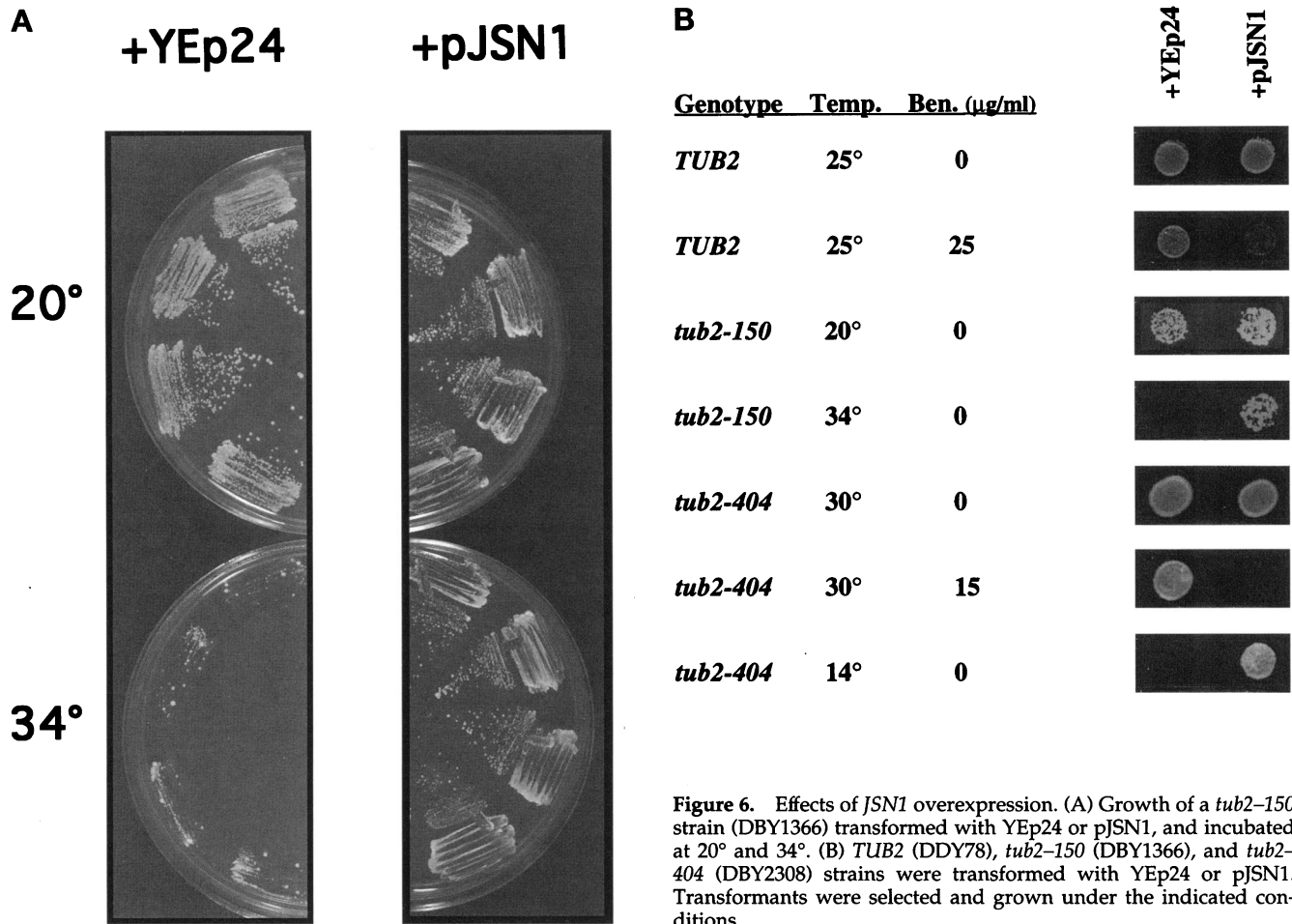
A

+YEp24   +pJSN1

20°

34°

B

Genotype	Temp.	Ben. (μg/ml)	+YEp24	+pJSN1
TUB2	25°	0		
TUB2	25°	25		
tub2-150	20°	0		
tub2-150	34°	0		
tub2-404	30°	0		
tub2-404	30°	15		
tub2-404	14°	0		

Figure 6. Effects of *JSN1* overexpression. (A) Growth of a *tub2–150* strain (DBY1366) transformed with YEp24 or pJSN1, and incubated at 20° and 34°. (B) *TUB2* (DDY78), *tub2–150* (DBY1366), and *tub2–404* (DBY2308) strains were transformed with YEp24 or pJSN1. Transformants were selected and grown under the indicated conditions.

protein, without significant similarity to any known protein. However, one region of Jsn1p was found to share significant similarity with several proteins.

Three stretches of sequence lying between residues 625 and 706 show significant similarity to the Pumilio domain, a group of eight tandem repeats named after the first protein with this domain to be identified (Figure 8B) (Barker *et al.*, 1992; Macdonald, 1992). Pumilio is a large protein consisting primarily of homopolymeric stretches of amino acids and the Pumilio domain, and is required for abdominal pattern formation in embryos of *Drosophila melanogaster*. The details of Pumilio's function are unknown, but it has been found to bind to the NRE (nanos responsive element) sequence found in *hunchback* mRNA (Murata and Wharton, 1995). Regulated translation of *hunchback* mRNA is necessary for proper segmentation of the *Drosophila* embryo (Barker *et al.*, 1992).

Pumilio domain-containing proteins have been found in yeast, worms, and humans. Two proteins containing Pumilio domains have been found in

yeast. *YGL023* was found as part of a genome sequencing project, and its function is unknown (Chen *et al.*, 1991). *HTR1* encodes a protein of unknown function required for efficient growth at high temperature and recovery from mating pheromone-induced arrest (Kikuchi *et al.*, 1994).

In contrast to the previously identified Pumilio domain-containing proteins, Jsn1p contains only three convincing iterations of the repeat, as seen in Figure 8B. Also, Jsn1p's repeats are not as conserved as the repeats of the other proteins. However, when Jsn1p's Pumilio domain-region is used to retrieve similar sequences from GenBank using the blastp program, only Pumilio domain-containing proteins are found to have significant similarity. Three orders of magnitude separate the Smallest Sum Probability (P(N)) scores for Pumilio and for the most similar non-Pumilio domain-containing protein. Jsn1p also contains two asparagine-rich regions between residues 507–518 and 1065–1076, a feature common to several of the Pumilio domain-containing proteins. With the exception of Pumilio and the

Table 4. Effects of *JSN1* overexpression on the phenotypes of a collection of microtubule-affecting mutations

Strain	Mutation	Phenotype[a]	Phenotype with pJSN1[b]
DDY78	wild type	normal	ben[ss]
DBY1366	tub2-150	Ts[-]; ben[D]; short spindle; excess MTs[c]	Ts[-] suppressed
DBY2395	tub1-501	ben[ss]; Ts[-]; ab. MTs Cs[-]; few MTs[d]	—
DBY2397	tub1-603	ben[ss]; Ts[-]; ab. MTs[d]	—
DBY2400	tub1-705	Cs[-]; ben[ss]; ab. MTs[d]	—
DBY2402	tub1-713	Cs[-]; ben[ss]; few MTs[d]	—
DBY2403	tub1-714	Cs[-]; ben[ss]; ab. MTs; excess MTs[d]	—
DBY2404	tub1-716	Cs[-]; ben[ss d]	—
DBY2406	tub1-719	Cs[-]; ben[ss]; ab. MTs[d]	—
DBY2416	tub1-737	Cs[-]; short spindle[d]	—
DBY2431	tub1-764	Cs[-]; ab. MTs[d]	—
DBY2304	tub2-402	Cs[-]; ben[R]; few MTs[e]	—
DBY2305	tub2-403	Cs[-]; ben[ss]; no MTs[e]	—
DBY2308	tub2-404	Cs[-]; short spindle[e]	ben [ss f]; Cs[-] suppressed
DBY2309	tub2-405	Cs[-]; ben[ss]; few MTs; ab. MTs[e]	—
DBY3393	cin1::HIS3	Cs[-]; extreme ben[ss g]	—
DBY3424	cin2-1	Cs[-]; extreme ben[ss g]	—
DBY3391	cin2::LEU2	Cs[-]; extreme ben[ss g]	—
DBY5284	cin4-4	Cs[-]; extreme ben[ss g]	—

Each strain was transformed with pJSN1 and with Yep24 (as a control) and plated under that strain's permissive conditions. Two colonies from each transformation were picked and plated using a 32-prong inoculator onto SD medium with or without benomyl. A variety of incubation temperatures and benomyl concentrations were used, as follows: 37°, no benomyl; 36°, no benomyl; 30°, 0, 0.5, 5, 10, 25, and 50 μg/ml benomyl; 25°, 0, 0.5, 5, 10, 15, 25, and 50 μg/ml benomyl; 20°, 0, 0.5, 5, 10, 15, and 25 μg/ml benomyl; 14°, no benomyl.

[a] Ts[-], unable to grow at 34° or 37°; Cs[-], unable to grow at 16°, 14°, or 11°; ben[ss], inhibited for growth by 5-25 μg/ml benomyl at 25°; extreme ben[ss], inhibited for growth by less than 5 μg/ml benomyl at 25°; ben[R], able to grow on greater than 25 μg/ml benomyl at 25°; ben[D], requires benomyl for growth above 25°; short spindle, at nonpermissive temperature cannot elongate spindle; few MTs, under nonpermissive conditions, has too few microtubules; excess MTs, under nonpermissive conditions, has too many microtubules; ab. MTs, under nonpermissive conditions, has abnormal or disorganized microtubule structures.

[b] suppressed, plasmid suppresses the growth defects associated with that mutation; —, plasmid causes a small increase in the benomyl sensitivity of this strain, similar to its effect on wild-type strains, or does not alter its growth characteristics.

[c] (Thomas *et al.*, 1985); this study.

[d] (Schatz *et al.*, 1988).

[e] (Huffaker *et al.*, 1988).

[f] At permissive temperature (Figure 6B).

[g] (Stearns *et al.*, 1990).

Pumilio domain protein from humans, these proteins do not share any similarity outside of the repeat region. Thus, although Jsn1p appears to contain a Pumilio domain, it is a unique, and perhaps distantly related, one.

Construction and Analysis of a Strain Lacking JSN1

A strain lacking *JSN1* was created by replacing the *JSN1* open reading frame using a plasmid designed for that purpose, to create a diploid heterozygous at the *JSN1* locus. This diploid is viable and has no obvious growth defects. When sporulated and subjected to tetrad analysis, all four spores from the heterozygote are viable, and the *LEU2* gene, used to mark the *jsn1* disruption, segregates 2:2. Cells from spore colonies from a number of tetrads were grown on plates containing rich medium, with or without added benomyl, and incubated at a range of temperatures from 14–37°. In no instance did the phe-notype of the *jsn1* cells differ from that of their *JSN1* siblings.

The *jsn1::LEU2*-containing strain was crossed to a *tub2-150::HIS3* strain. The double-heterozygote thus constructed is viable and has growth properties similar to those of a *tub2-150/+* strain (*tub2-150* is semi-dominant; i.e., heterozygous strains are more resistant to benomyl than wild-type diploids). This diploid, when sporulated and dissected, typically yields four viable spores, two of which grow well at 20° and two of which grow slowly. Invariably, the slow-growing spore colonies carry the *tub2-150::HIS3* mutation. Tetrads with one or two dead spores are sometimes obtained. The segregation of nutritional markers among the living spore colonies can be used to infer that the dead spores always carry *tub2-150::HIS3* (the *tub2-150* mutation, even under permissive conditions, results in moderate levels of spore lethality [our unpublished ob-
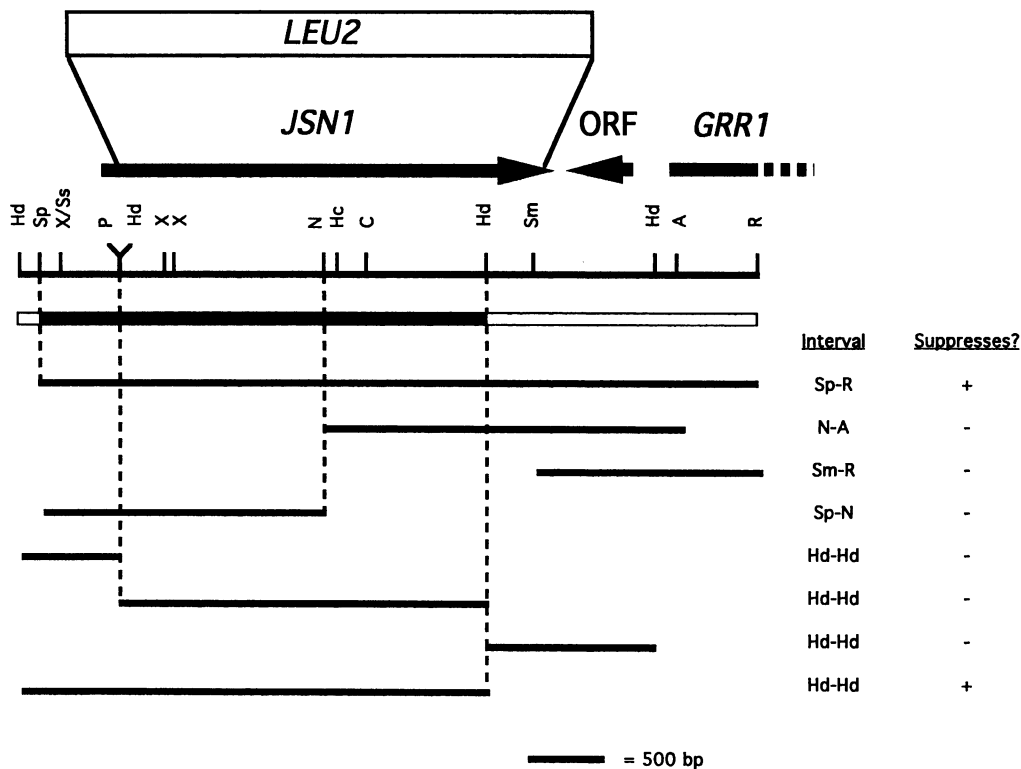
LEU2

JSN1 | ORF | GRR1

Interval	Suppresses?
Sp-R	+
N-A	-
Sm-R	-
Sp-N	-
Hd-Hd	-
Hd-Hd	-
Hd-Hd	-
Hd-Hd	+

= 500 bp

Figure 7. Restriction map and deletion of *JSN1*. Restriction map of the 5-kb *JSN1*-containing region. Above the restriction map, open reading frames are indicated with arrows (see text). Black lines below the restriction map indicate restriction fragments that were tested for the ability to suppress *tub2–150* in high copy number. To their right is listed each fragment's identity, and whether or not it could suppress *tub2–150*. The bar directly below the restriction map shows, based on the results of this suppression analysis, where the suppressing activity is. These results show that the suppressing activity must extend from some point in the left-hand stippled area, through the black region, to some point in the right-hand stippled area. Only one open reading frame meets this criterion, the one labeled *JSN1*. Above the open reading frames, the *jsn1::LEU2* deletion construct is diagrammed. The *LEU2*-containing insert is not drawn to scale; it is actually 5.5 kb. Restriction enzyme abbreviations are as follows: A, *ApaI*; C, *ClaI*; Hc, *HincII*; Hd, *HindIII*; N, *NcoI*; P, *PstI*; R, *EcoRI*; Sm, *SmaI*; Ss, *SspI*; X, *XhoI*.

servations]). *jsn1::LEU2*, in contrast, is not preferentially associated with spore lethality or the slow growth phenotype.

The benomyl and temperature sensitivities of *tub2–150::HIS3, jsn1::LEU2* and *tub2–150::HIS3, JSN1* haploids were compared, and found to be indistinguishable. Similarly, microtubules in *JSN1* and *jsn1::LEU2* cells were compared using immunofluorescence microscopy, without any differences being seen.

Thus, although overexpression of *JSN1* apparently destabilizes microtubules, absence of *JSN1* is not lethal, even in a *tub2–150* background, and does not obviously affect the microtubule cytoskeleton.

JSN1 and *YGL023* Are Not Functional Homologues

Given that *JSN1* shares similarity with other yeast genes, and that the *jsn1* null allele does not cause a change in phenotype, it is possible that *JSN1* and one or more of these genes share redundant or overlapping functions. This possibility was examined using *YGL023*, the first yeast gene encoding a Pumilio domain protein to be characterized. As with *JSN1*, a disruption of *YGL023* was reported to be viable (Chen *et al.*, 1991). However, the reported

YGL023 disruption is predicted to leave the N-terminal 80% of the protein intact. This much of the protein might retain some or all of the activity of the wild-type protein. A more complete disruption of *YGL023* was therefore constructed as described in MATERIALS AND METHODS. This disruption is not lethal, and does not cause a change in benomyl or temperature sensitivity.

The *YGL023* disruption was crossed into a *JSN1*-disrupted background. A diploid strain doubly heterozygous for these two mutations is viable and sporulates efficiently. Tetrad analysis of spores revealed that virtually all spores are viable, including those containing both deletions. These double mutant spores also behave like wild-type cells in terms of their temperature and benomyl sensitivities. Thus, either *JSN1* and *YGL023* do not encode proteins with redundant functions, or one or more additional genes exist that encode functions redundant with these two genes (see DISCUSSION).

Finally, the ability of *YGL023* to act as a high-copy number suppressor of *tub2–150* was tested. A *YGL023*-containing 2μ plasmid was constructed and introduced into a *tub2–150* strain. The *YGL023* plasmid does not suppress *tub2–150*.

A

```
   1 MDKSKQMNINNLSNIPEVIDPGITIPIYEEEYENNGESNSQLQQQPQKLGSYRS

  55 RAGKFSNTLSNLLPSISAKLHHSKKNSHGKNGAEFSSSNNSSQSTVASKTPRAS

 109 PSRSKMMESSIDGVIMDRPGSLTPPQDMEKLVHFPDSSNNFLIPAPRGSSDSFN

 163 LPHQISRTRNNIMSSQITSISSIAPKPRTSSGIWSSNASANDPMQQHLLQQLQP

 217 TTSNNTINSNTLNDYSTKTAYFINMVSTSGSGQMADNKMNINNLAIPNSVWSNIR

 271 QRSQSNASSIYTDAPLYEQPARASISSHYTIPTQESPLIADEIDPQSINWVIMD

 325 PTVPSINQISNLLPINTISISNVFPLQHQQPQLNNAINLTSTSLATLCSKYGEV

 379 ISARTLRNLNMALVEFSSVESAVKALDSLQGKEVSMIGAPSKISFAKILPMHQQ

 433 PPQFLLNSQGLPLGLENNNLQPQPLLQEQLFNGAVTFQQQGNVSIPVFNQQSQQ

 487 SQHQNHSSGSAGFSNVLHGYNNNNSMHGNNNNSANEKEQCPFPLPPPNVNEKED

 541 LLREIIELFEANSDEYQINSLIKKSLNHKGTSDTQNFGPLPEPLSGREFDPPKL

 595 RELRKSIDSNAFSDLEIBQLAIAMLDELPELSSDYLGNTIVQKLFEHSSDIIKD

 649 IMLRKTSKYLTSMGVHKNGIWACQKMITMAHTPRQIMQVTQGVKDYCTPLINDQ

 703 FGNYVIQCVLKFGFPWNQFIFESIIANFWVIVQNRYGARAVRACLEAHDIVTPE

 757 QSIVLSAMIVTYAEYLSTNSNGALLVIWFLDTSVLPNRHSILAPRLTKRIVELC

 811 GHRLASLTILKVLNYRGDDNARKIILDSLFGNVNAHDSSPPKELTKLLCETNYG

 865 PTFVHKVLAMPLLEDDLRAHIIKQVRKVLITDSTQIQPSRRLLEEVGLASPSSTH

 919 NKTKQQQQQHHNSSISHMFATPDTSGQHMRGLSVSSVKSGGSKHTIMNTTTING

 973 SSASTLSPGQPLNANSNSSMGYFSYPGVFPVSGFSGNASNGYAMNNDDLSSQFD

1027 MLNFNNGTRLSLPQLSLINHNNTTMELVNNVGSSQPHINNNNNNNNINYNDDNT

1081 VFETLTLHSAN
```

B

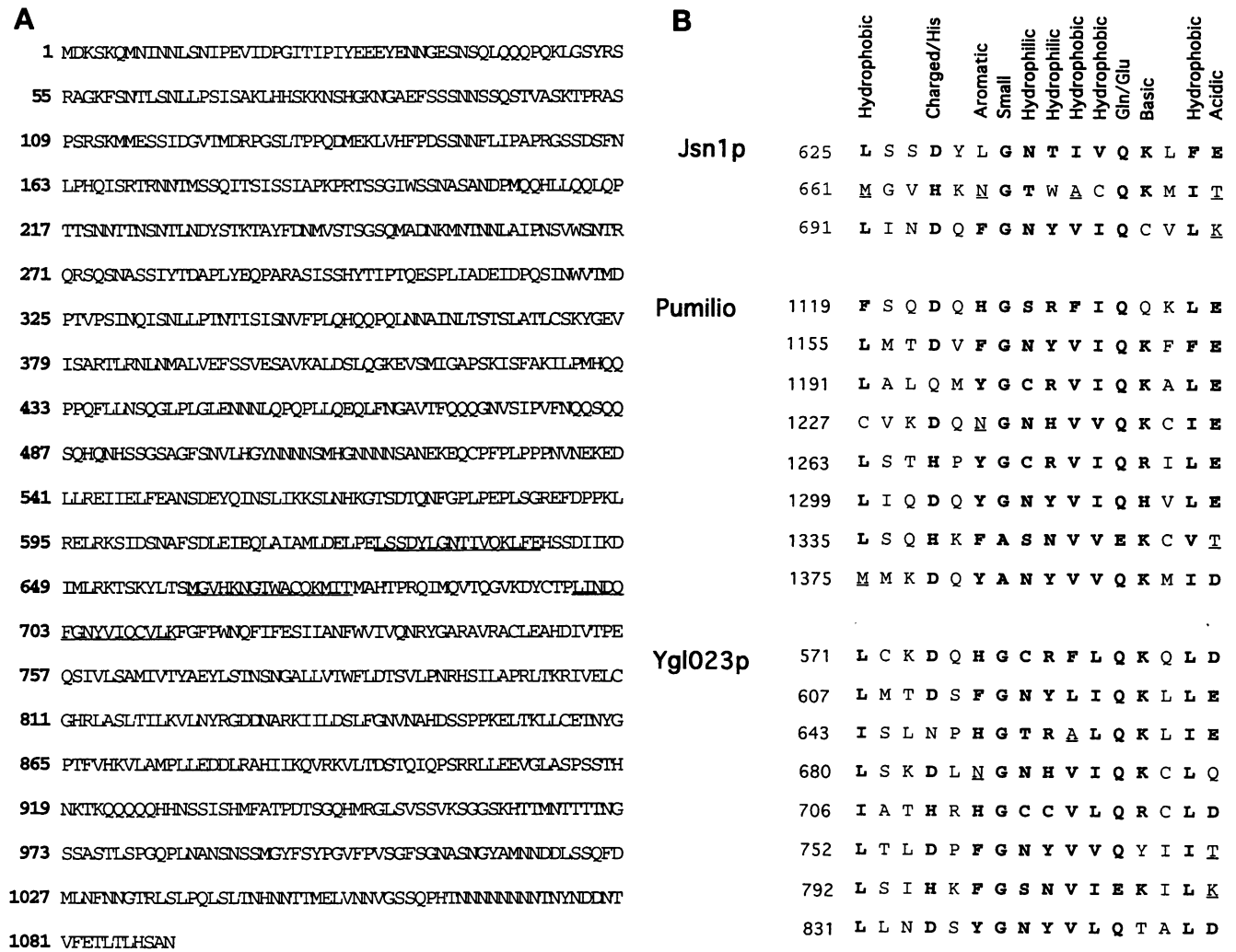|		Hydrophobic	Charged/His	Aromatic	Small	Hydrophilic	Hydrophilic	Hydrophobic	Hydrophobic	Gln/Glu	Basic	Hydrophobic	Acidic
Jsn1p	625	L	S S	D	Y L	G	N	T	I	V Q	K	L	F E
	661	M	G V H	K	N G	T	W	A	C	Q K	M	I	T
	691	L	I N	D	Q F	G	N	Y	V	I Q	C	V	L K
Pumilio	1119	F	S Q	D	Q H	G	S	R	F	I Q	Q	K	L E
	1155	L	M T	D	V F	G	N	Y	V	I Q	K	F	F E
	1191	L	A L	Q	M Y	G	C	R	V	I Q	K	R	A L E
	1227	C	V K	D	Q N	G	N	H	V	V Q	K	C	I E
	1263	L	S T	H	P Y	G	C	R	V	I Q	R	I	L E
	1299	L	I Q	D	Q Y	G	N	Y	V	I Q	H	V	L E
	1335	L	S Q	H	K F	A	S	N	V	V E	K	C	V T
	1375	M	M K	D	Q Y	A	N	Y	V	V Q	K	M	I D
Ygl023p	571	L	C K	D	Q H	G	C	R	F	L Q	K	Q	L D
	607	L	M T	D	S F	G	N	Y	L	I Q	K	L	L E
	643	I	S L	N	P H	G	T	R	A	L Q	K	L	I E
	680	L	S K	D	L N	G	N	H	V	I Q	K	C	L Q
	706	I	A T	H	R H	G	C	C	V	L Q	R	C	L D
	752	L	T L	D	P F	G	N	Y	V	V Q	Y	I	I T
	792	L	S I	H	K F	G	S	N	V	I E	K	I	L K
	831	L	L N	D	S Y	G	N	Y	V	L Q	T	A	L D

Figure 8. Sequence of Jsn1p. (A) Predicted amino acid sequence of Jsn1p. Standard one-letter amino acid abbreviations are used. Regions showing similarity to the Pumilio domain (see text) are underlined. The GenBank accession number is L43493. (B) Alignment of similar sequences from Jsn1p, Pumilio, and Ygl023p. Residues matching the consensus sequence are in bold type. Residues not matching the consensus, but present in Jsn1p and in either or both of the other two proteins at the same position in one or more repeat, are underlined. Pumilio domain consensus adapted from Barker *et al.* (1992).

Analysis of Jsn1p

A *JSN1* and *E. coli trpE* gene fusion was constructed in the pATH11 vector. This fusion protein was used to produce anti-Jsn1p antibodies in rabbits. Immunoblot analysis using these antibodies shows the presence, in wild-type yeast extracts, of a protein with an apparent molecular mass of 125 kDa, close to that predicted for Jsn1p (Figure 9A). This protein is present at greatly elevated levels in strains that overexpress *JSN1*, and is absent from *jsn1*-deleted strains. Therefore, the protein recognized by these antibodies is Jsn1p.

Affinity-purified anti-Jsn1p antibodies were used to determine the cellular location of Jsn1p using immunofluorescence microscopy. In wild-type cells, subjected to a variety of treatments to enhance stain-ing, only very faint staining of Jsn1p was achieved. However, strains overexpressing *JSN1* are brightly stained by the antibodies. As shown in Figure 9B, Jsn1p is located in discreet patches uniformly distributed over the surface of cells during all phases of the cell cycle. The staining pattern in the Jsn1p-overexpressing strain is qualitatively similar to the staining in the strain expressing normal levels of Jsn1p, but is much more intense.

DISCUSSION

Analysis of the tub2-150 Mutation

A single amino acid change, $\text{Thr}_{238} \rightarrow$ Ala, is the *tub2-150* mutation. This threonine is conserved be-
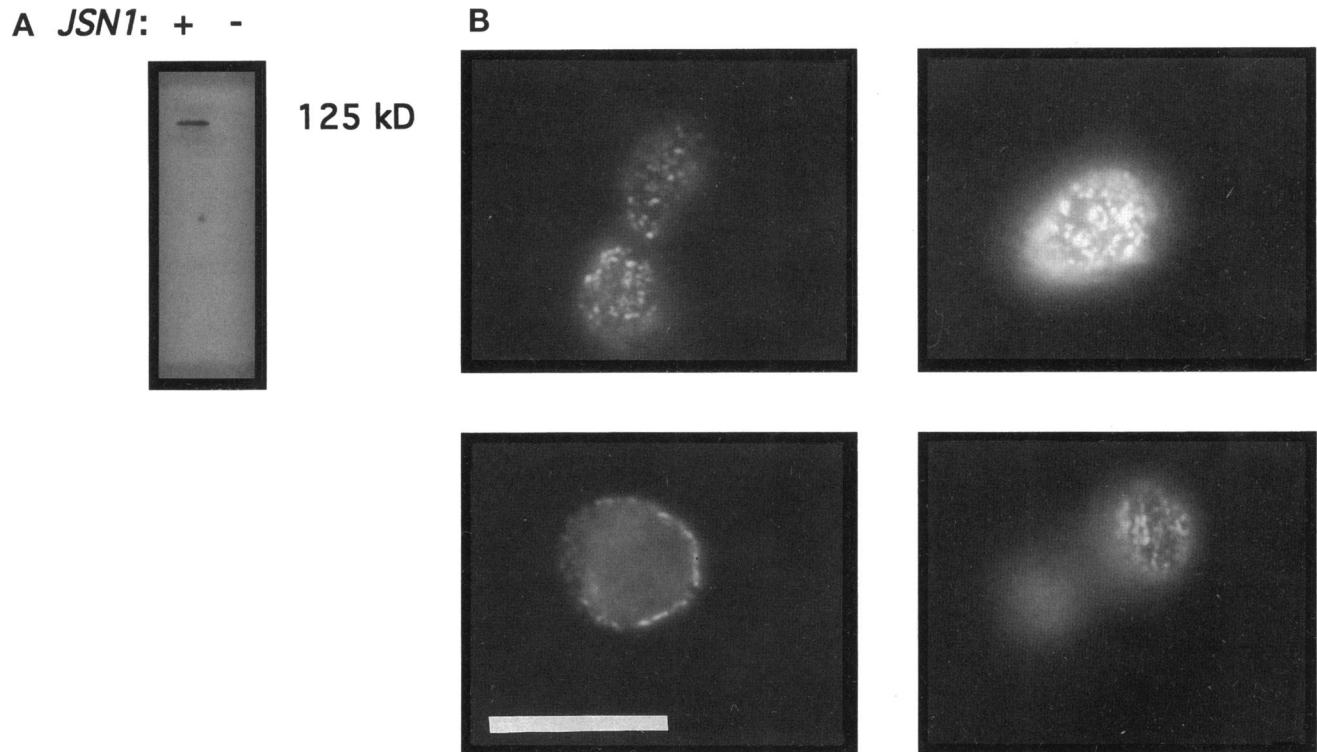
Figure 9. Western analysis and immunofluorescence using the anti-Jsn1p antibody. Polyclonal antibodies recognizing Jsn1p were produced as described in MATERIALS AND METHODS. (A) PAGE-separated whole cell extracts from *jsn1::LEU2* cells (strain DDY835) and *JSN1* cells (strain DDY836) were probed with the anti-Jsn1p antibodies. A band of 125 kD was detected in the *JSN1* but not the *jsn1::LEU2* strain. (B) Strain DDY110 was transformed with pJSN1 and prepared for immunofluorescence as described in MATERIALS AND METHODS. Focal planes were chosen to highlight the localization of Jsn1p protein in this *JSN1* overexpressing strain to the cell perimeter. Because of the effects of photobleaching, each image is of a different cell. When individual cells are examined microscopically, we observe that it is the perimeter of each cell that is stained, never the interior. Bar, 10 μm.

tween β-tubulins in fungi and metazoa, but protozoa, ·plants, and algae typically contain a cysteine in this position, and α-tubulins contain either leucine or isoleucine at their analogous position (Burns and Surridge, 1994). Very little is known about the contribution of individual amino acid residues to the structure or function of the tubulins, making it difficult to assess the significance of this finding. Threonines are the targets of a number of protein kinases, and at least some β-tubulins are phosphorylated on certain residues under certain conditions (Pallas and Solomon, 1982; Gard and Kirschner, 1985). However, no data exist to suggest β-tubulin Thr_{238} is phosphorylated in any organism, and we found no evidence of altered electrophoretic mobility of β-tubulin in *tub2–150* cells.

Because of the complex nature of microtubule dynamics, one can imagine a number of ways in which these dynamics could be perturbed by a tubulin mutation like *tub2–150*. The structure of the microtubule lattice is such that each tubulin heterodimer is thought to make extensive contacts with other tubulins (Nogales *et al.*, 1995). In principle, a mutation that increased the stability of microtubules could do so by increasing the strength of any one of these interactions.

Another possibility is that the *tub2–150* mutation reduces the rate of hydrolysis of the exchangeable GTP bound to the β-tubulin of each tubulin heterodimer, increasing the size of the postulated GTP cap, and thereby reducing the frequency of catastrophe and/or increasing the probability of transition between catastrophe and rescue. Whether *tub2–150* acts in this way or not, there is experimental evidence to support such a possibility. Site-directed mutagenesis was used to create a series of yeast β-tubulin mutants altering residues that might be involved in GTP hydrolysis. Biochemical characterization of these mutants showed a correlation between increased GTP hydrolysis and increased dynamic instability (Davis *et al.*, 1994). Similarly, a biochemical analysis of *tub2–150* tubulin, now underway, will allow us to determine which assembly parameters, if any, are affected by this mutation.

The *tub2–150* mutation might alter microtubule dynamics less directly, by altering the interaction of nontubulin regulators of microtubule stability with micro-

tubules. For example, tub2–150 microtubules might be less susceptible to a microtubule severing activity of the type described in frogs and sea urchins (Vale, 1991; McNally and Vale, 1993; Shiina et al., 1994), or be a poor substrate for the minus-end depolymerizing activity of Kar3p (Endow et al., 1994). Conversely, tub2–150 microtubules could be more susceptible to the activity of a protein that stabilizes microtubules.

One intriguing property of the tub2–150 defect is the number of ways it can be suppressed: by incubation at low temperature, by application of microtubule depolymerizing drugs, or by mutations in other genes. It is likely that these conditions affect microtubules in distinct ways. Changes in microtubule stability caused by changes in temperature are probably due to the cold-sensitive nature of the hydrophobic effect, while benomyl likely acts via mass action by sequestering tubulin heterodimers. How cin mutations suppress tub2–150 is unknown, but this suppression might represent a third mechanism. This suggests that it is an intrinsic property of tub2–150 microtubules that must be remedied (e.g., their increased stability), rather than a defect in a specific molecular interaction. Therefore, there might be a number of genetic perturbations that lead to suppression.

The tub2–150 phenotype is reminiscent of the effects of the microtubule-stabilizing drug taxol. Like tub2–150 cells under nonpermissive conditions, tissue culture cells treated with taxol fail to complete mitosis (Jordan et al., 1993). Taxol is an effective chemotherapeutic agent against a number of different aggressive cancers (Guchelaar et al., 1994). As taxol does not affect S. cerevisiae microtubules (Barnes et al., 1992), the genetic, molecular, and biochemical characterization of tub2–150 microtubules may offer unique insights into the mode of action of this important drug.

JSN1 Encodes a Unique Protein

JSN1 is predicted to encode a protein that is unique throughout most of its length. That Jsn1p contains a region similar to the tandem repeats found in the Pumilio domain is not informative, as the functions of these repeats are unknown. Pumilio, the best studied of these proteins, has recently been found to bind to the NRE, a sequence found within the hunchback mRNA (Murata and Wharton, 1995). As a truncation of Pumilio lacking the Pumilio domain binds the NRE, there is little reason to believe that the Pumilio domain is an RNA binding motif (Murata and Wharton, 1995).

Our demonstration that Jsn1p is dispensable under all conditions assayed prompted us to determine whether Ygl023p, which also contains a Pumilio domain, is a functional homologue of Jsn1p. Although Jsn1p and Ygl023p apparently do not share redundant functions, the possibility exists that Jsn1p homologues are encoded by other genes.

Suppression of tub2–404 by JSN1 Overexpression

Overexpression of JSN1 was able to suppress only one other mutation, tub2–404. At first glance, tub2–150 and tub2–404 would appear to be very dissimilar mutations. In contrast to the heat-sensitive benomyl-dependence of tub2–150, the tub2–404 mutation causes a cold-sensitive growth defect, and does not affect benomyl sensitivity (Huffaker et al., 1988). The amino acid changes in these two mutants lie in different parts of the β-tubulin sequence (Huffaker et al., 1988, and this report). However, immunofluorescence analysis shows that both of these mutants, under their nonpermissive conditions, arrest with short spindles (Huffaker et al., 1988, and this report). It is possible that both mutations cause a conditional increase in microtubule stability that JSN1 overexpression suppresses, perhaps by causing an increase in microtubule dynamics. Alternatively, it is possible that tub2–150 and tub2–404 cause spindle elongation defects for different reasons, and that JSN1 acts not to alter microtubule stability, but rather to promote anaphase (see below).

If JSN1 can suppress two mutations that cause a spindle elongation defect, why can't it suppress others? The tub1–737 mutation imparts a phenotype very similar to that of tub2–404 (Schatz et al., 1988): wild-type benomyl sensitivity, cold-sensitive growth, and a spindle elongation defect at low temperature. The suppression of tub2–404 by JSN1 overexpression is somewhat weaker than the suppression of tub2–150. This might indicate that tub2–404 at 14° has a more severe defect than tub2–150 has at 34°. Perhaps tub1–737 has an even more severe defect. Alternatively, the tub1–737 defect may be fundamentally different from those of the two TUB2 mutants, and so not subject to JSN1 dosage suppression.

Models for Suppression of tub2–150 by JSN1

The most obvious model for JSN1 suppression of tub2–150 is through direct contact with microtubules or tubulin, where it could affect any one of the parameters possibly affected by tub2–150 (listed above). Immunofluorescence, using an anti-Jsn1p antibody to stain cells overexpressing JSN1, revealed brightly staining dots of Jsn1p uniformly distributed across the cell cortex. Thus, if Jsn1p does interact with microtubules, it must do so at levels that escape detection, or only at the ends of microtubules, as a component of the kinetochore or spindle pole body, where it might be very difficult to detect using immunofluorescence. It is possible that Jsn1p binds to unpolymerized tubulin, sequestering it into a pool that is unavailable for assembly, thereby employing the law of mass action to effect microtubule disassembly.

Another possibility is that Jsn1p functions as part of an apparatus that coordinates the microtubule cytoskeleton with the cell cycle. In this model, tub2–150

and *tub2–404* cells can be "pushed" through anaphase by overexpressing *JSN1*. The stability of microtubules would not be directly affected by Jsn1p. This also accounts for the localization of Jsn1p at the cell cortex, because a signal-sending molecule would not necessarily have to interact directly with microtubules. It would also account for the relatively small increase in benomyl sensitivity (compared with that caused by mutations in the *CIN* genes) caused by overexpressing *JSN1* in an otherwise wild-type background because cells might only be sensitive to the *JSN1*-dependent signal during a restricted part of the cell cycle.

A more complete understanding of both the *tub2–150* phenotype and of *JSN1* will be afforded by a biochemical analysis of *tub2–150* tubulin and characterization of the other suppressors to come out of our selection. Taken together, these experiments will allow us to identify those microtubule assembly parameters affected by *tub2–150*, to correlate biochemical defects with the observed behavior of *tub2–150* mutants, and to design experiments to test the role of *JSN1* and the other suppressors in both wild-type and *tub2–150* cells.

ACKNOWLEDGMENTS

REFERENCES

Amin-Hanjani, S., and Wadsworth, P. (1991). Inhibition of spindle elongation by taxol. Cell. Motil. Cytoskeleton 20, 136–144.

Ausubel, F.M., Brent, R., Kingston, R.E., Moore, D.D., Seidman, J.G., Smith, J.A., and Struhl, K. (1989). Short Protocols in Molecular Biology, New York: Greene Publishing Associates and Wiley-Interscience.

Baas, P.W., Slaughter, T., Brown, A., and Black, M.M. (1991). Microtubule dynamics in axons and dendrites. J. Neurosci. Res. 30, 134–153.

Barker, D.D., Wang, C., Moore, J., Dickinson, L.K., and Lehmann, R. (1992). Pumilio is essential for function but not for distribution of the Drosophila abdominal determinant Nanos. Genes Dev. 6, 2312–2326.

Barnes, G., Drubin, D.G., and Stearns, T. (1990). The cytoskeleton of Saccharomyces cerevisiae. Curr. Opin. Cell. Biol. 2, 109–115.

Barnes, G., Louie, K.A., and Botstein, D. (1992). Yeast proteins associated with microtubules in vitro and in vivo. Mol. Biol. Cell 3, 29–47.

Belmont, L.D., Hyman, A.A., Sawin, K.E., and Mitchison, T.J. (1990). Real-time visualization of cell cycle-dependent changes in microtubule dynamics in cytoplasmic extracts. Cell 62, 579–589.

Bollag, D.M., Tornare, I., Stalder, R., Doret, A.M.P., Rozycki, M.D., and Edelstein, S.J. (1990). Overexpression of tubulin in yeast, differences in subunit association. Eur. J. Cell Biol. 51, 295–302.

Burke, D., Gasdaska, P., and Hartwell, L. (1989). Dominant effects of tubulin overexpression in Saccharomyces cerevisiae. Mol. Cell. Biol. 9, 1049–1059.

Burns, R.G., and Surridge, C.D. (1994). Tubulin: conservation and structure. In: Microtubules, New York: Wiley-Liss, 3–31.

Byers, B., and Goetsch, L. (1975). Behavior of spindles and spindle plaques in the cell cycle and conjugation of Saccharomyces cerevisiae. J. Bacteriol. 124, 511–523.

Byers, B., Shriver, K., and Goetsch, L. (1978). The role of spindle pole bodies and modified microtubule ends in the initiation of microtubule assembly in Saccharomyces cerevisiae. J. Cell Sci. 30, 331–352.

Carlson, M., and Botstein, D. (1982). Two differentially regulated mRNAs with different 5′ ends encode secreted and intracellular forms of invertase. Cell 28, 145–154.

Cassimeris, L.U., Pryer, N.K., and Salmon, E.D. (1988). Real-time observations of microtubule dynamic instability in living cells. J. Cell Biol. 107, 2223–2231.

Chen, W., Balzi, E., Capieaux, E., and Goffeau, A. (1991). The YGL023 gene encodes a putative regulatory protein. Yeast 7, 309–312.

Davis, A., Sage, C.R., Dougherty, C.A., and Farrell, K.W. (1994). Microtubule dynamics modulated by guanosine triphosphate hydrolysis activity of β-tubulin. Science 264, 839–842.

Davis, A., Sage, C.R., Wilson, L., and Farrel, K.W. (1993). Purification and biochemical characterization of tubulin from the budding yeast Saccharomyces cerevisiae. Biochemistry 32, 8823–8835.

Drubin, D.G., Miller, K.G., and Botstein, D. (1988). Yeast actin-binding proteins: evidence for a role in morphogenesis. J. Cell Biol. 107, 2551–2561.

Endow, S.A., Kang, S.J., Satterwhite, L.L., Rose, M.D., Skeen, V.P., and Salmon, E.D. (1994). Yeast Kar3p is a minus-end microtubule motor protein that destabilizes microtubules preferentially at the minus ends. EMBO J. 13, 2708–2713.

Eshel, D., Urrestarazu, L.A., Vissers, S., Jauniaux, J.C., Vleit-Reedijk, J.C.v., Planta, R.J., and Gibbons, I.R. (1993). Cytoplasmic dynein is required for normal nuclear segregation in yeast. Proc. Natl. Acad. Sci. USA 90, 11172–11176.

Flick, J.S., and Johnston, M. (1991). GRR1 of Saccharomyces cerevisiae is required for glucose repression and encodes a protein with leucine-rich repeats. Mol. Cell. Biol. 11, 5101–5112.

Gard, D.L., and Kirschner, M.W. (1985). A polymer-dependent increase in phosphorylation of β-tubulin accompanies differentiation of a mouse neuroblastoma cell line. J. Cell Biol. 100, 764–774.

Guchelaar, H.J., Napel, C.H.t., Vries, E.G.d., and Mulder, N.H. (1994). Clinical, toxicological and pharmaceutical aspects of the antineoplastic drug taxol: a review. Clin. Oncol. (Roy. Coll. Radiol.) 6, 40–48.

Horio, T., and Hotani, H. (1986). Visualization of the dynamic instability of individual microtubules by dark-field microscopy. Nature 321, 605–607.

Hoyt, M.A., He, L., Loo, K.K., and Saunders, W.S. (1992). Two Saccharomyces cerevisiae kinesin-related gene products required for mitotic spindle assembly. J. Cell Biol. 118, 109–120.

Hoyt, M.A., He, L., Totis, L., and Saunders, W.S. (1993). Loss of function of *Saccharomyces cerevisiae* kinesin-related *CIN8* and *KIP1* is suppressed by *KAR3* motor domain mutations. Genetics *135*, 35–44.

Hoyt, M.A., Totis, L., and Roberts, B.T. (1991). *S. cerevisiae* genes required for cell cycle arrest in response to loss of microtubule function. Cell *66*, 507–517.

Huffaker, T.C., Hoyt, M.A., and Botstein, D. (1987). Genetic analysis of the yeast cytoskeleton. Annu. Rev. Genet. *21*, 259–284.

Huffaker, T.C., Thomas, J.H., and Botstein, D. (1988). Diverse effects of β-tubulin mutations on microtubule formation and function. J. Cell Biol. *106*, 1997–2010.

Hutter, K.J., and Eipel, H.E. (1978). Flow cytometric determinations of cellular substances in algae, bacteria, molds and yeast. Antonie Leeuwenhoek J. Microbiol. Ser. *44*, 269–282.

Hyams, J.S., and Lloyd, C.W. (1994). Microtubules, New York: Wiley-Liss.

Hyman, A.A., Salser, S., Drechsel, D.N., Unwin, N., and Mitchison, T.J. (1992). Role of GTP hydrolysis in microtubule dynamics: information from a slowly hydrolyzing analogue, GMPCPP. Mol. Biol. Cell *3*, 1155–1167.

Ito, H., Fukuda, Y., Murata, K., and Kimura, A. (1983). Transformation of intact yeast cells treated with alkali cations. J. Bacteriol. *153*, 163–168.

Jordan, M.A., Thrower, D., and Wilson, L. (1992). Effects of vinblastine, podophillotoxin, and nocodozole on mitotic spindles: implications for the role of microtubule dynamics in mitosis. J. Cell Sci. *102*, 401–416.

Jordan, M.A., Toso, R., Thrower, D., and Wilson, L. (1993). Mechanism of mitotic block and inhibition of cell proliferation by taxol at low concentrations. Proc. Natl. Acad. Sci. USA *83*, 9552–9556.

Katz, W., Weinstein, B., and Solomon, F. (1990). Regulation of tubulin levels and microtubule assembly in *Saccharomyces cerevisiae*, consequences of altered tubulin gene copy number. Mol. Cell. Biol. *10*, 5286–5294.

Kikuchi, Y., Oka, Y., Kobayashi, M., Uesono, Y., Toh-e, A., and Kikuchi, A. (1994). A new yeast gene, *HTR1*, required for growth at *h*igh *t*emperature, is needed for recovery from mating pheromone-induced G1 arrest. Mol. Gen. Genet. *245*, 107–116.

Kirschner, M., and Schulze, E. (1986). Morphogenesis and the control of microtubule dynamics in cells. J. Cell Sci. *5*, 293–310.

Koerner, T.J., Hill, J.E., Myers, A.M., and Tzagoloff, A. (1991). High-expression vectors with multiple cloning sites for construction of *trpE* fusion genes: pATH vectors. In: Guide to Yeast Genetics and Molecular Biology, vol. 194, San Diego: Harcourt Brace Jovanovich, 477–490.

Kristofferson, D., Mitchison, T., and Kirschner, M.W. (1986). Direct observation of steady-state microtubule dynamics. J. Cell Biol. *102*, 1007–1019.

Li, R., and Murray, A.W. (1991). Feedback control of mitosis of budding yeast. Cell *66*, 519–531.

Macdonald, P.M. (1992). The *Drosophila* pumilio gene: an unusually long transcription unit and an unusual protein. Development *114*, 221–232.

McNally, F.J., and Vale, R.D. (1993). Identification of katanin, an ATPase that severs and disassembles stable microtubules. Cell *75*, 419–429.

Meluh, P., and Rose, M.D. (1990). KAR3, a kinesin-related gene required for yeast nuclear fusion. Cell *60*, 1029–1041.

Mitchison, T., and Kirschner, M.W. (1984). Dynamic instability of microtubule growth. Nature *312*, 237–242.

Mitchison, T.J., and Salmon, E.D. (1992). Poleward kinetochore fiber movement occurs during both metaphase and anaphase-A in newt lung cell mitosis. J. Cell Biol. *119*, 569–582.

Murata, Y., and Wharton, R.P. (1995). Binding of Pumilio to maternal *hunchback* mRNA is required for posterior patterning in *Drosophila* embryos. Cell *80*, 747–756.

Nogales, E., Wolf, S.G., Khan, I.A., Ludueña, R.F., and Downing, K.H. (1995). Structure of tubulin at 6.5Å and location of the taxol-binding site. Nature *375*, 424–427.

Olson, M.V., Dutchik, J.E., Graham, M.Y., Brodeur, G.M., Helms, C., Frank, M., MacCollin, M., Scheinman, R., and Frank, T. (1986). Random-clone strategy for genomic restriction mapping in yeast. Proc. Natl. Acad. Sci. USA *83*, 7826–7830.

Pallas, D., and Solomon, F. (1982). Cytoplasmic microtubule-associated proteins: phosphorylation at novel sites is correlated with their incorporation into assembled microtubules. Cell *30*, 407–414.

Palmer, R.E., Sullivan, D.S., Huffaker, T., and Koshland, D. (1992). Role of astral microtubules and actin in spindle orientation and migration in the budding yeast, *Saccharomyces cerevisiae*. J. Cell Biol. *119*, 583–593.

Pfeffer, S.R., Drubin, D.G., and Kelly, R.B. (1983). Identification of three coated vesicle components as α- and β-tubulin linked to a phosphorylated 50,000-dalton polypeptide. J. Cell Biol. *97*, 40–47.

Pines, J., and Hunter, T. (1990). p34^{cdc2}: the S and M kinase? New Biol. *2*, 389–401.

Pringle, J.R., Adams, A.E., Drubin, D.G., and Haarer, B.K. (1991). Immunofluorescence methods for yeast. Methods Enzymol. *194*, 565–602.

Pringle, J.R., and Mor, J. (1975). Methods for monitoring the growth of yeast cultures and for dealing with the clumping problem. Methods Cell Biol. *11*, 131–168.

Roof, D.M., Meluh, P.B., and Rose, M.D. (1992). Kinesin-related proteins required for assembly of the mitotic spindle. J. Cell Biol. *118*, 95–108.

Rose, M.D., Winston, F., and Hieter, P. (1990). Methods in Yeast Genetics, Cold Spring Harbor, New York: Cold Spring Harbor Laboratory Press.

Salmon, E.D., Leslie, R.J., Saxton, W.M., Karow, M.L., and McIntosh, J.R. (1984). Spindle microtubule dynamics in sea urchin embryos: analysis using a fluorescein-labeled tubulin and measurement of fluorescence redistribution after laser photobleaching. J. Cell Biol. *99*, 2165–2174.

Sambrook, J., Fritsch, E.F., and Maniatis, T. (1989). Molecular Cloning: A Laboratory Manual, Cold Spring Harbor, New York: Cold Spring Harbor Laboratory Press.

Sammak, P.J., and Borisy, G.G. (1988). Direct observation of microtubule dynamics in living cells. Nature *332*, 724–726.

Sanger, F., Nicklen, S., and Coulsen, A.R. (1977). DNA sequencing with chain-terminating inhibitors. Proc. Natl. Acad. Sci. USA *74*, 5463–5467.

Saunders, W.S., and Hoyt, M.A. (1992). Kinesin-related proteins required for structural integrity of the mitotic spindle. Cell *70*, 451–458.

Saxton, W.M., and McIntosh, J.R. (1987). Interzone microtubule behavior in late anaphase and telophase spindles. J. Cell Biol. *105*, 875–886.

Schatz, P.J., Solomon, F., and Botstein, D. (1988). Isolation and characterization of conditional-lethal mutations in the *TUB1* α-tu-

bulin gene of the yeast *Saccharomyces cerevisiae*. Genetics *120*, 681–695.

Schiestl, R.H., and Gietz, R.D. (1989). High efficiency transformation of intact yeast cells using single stranded nucleic acids as a carrier. Curr. Genet. *16*, 339–346.

Schulze, E., and Kirschner, M.W. (1986). Microtubule dynamics in interphase cells. J. Cell Biol. *102*, 1020–1031.

Shelden, E., and Wadsworth, P. (1990). Interzonal microtubules are dynamic during spindle elongation. J. Cell Sci. *97*, 273–281.

Shiina, N., Gotoh, Y., Kubomura, N., Iwamatsu, A., and Nishida, E. (1994). Microtubule severing by elongation factor 1α. Science *266*, 282–285.

Sikorski, R.S., and Hieter, P. (1989). A system of shuttle vectors and yeast host strains designed for efficient manipulation of DNA in *Saccharomyces cerevisiae*. Genetics *122*, 19–27.

Southern, E. (1975). Detection of specific sequences among DNA fragments separated by gel electrophoresis. J. Mol. Biol. *98*, 503–517.

Stearns, T., and Botstein, D. (1988). Unlinked noncomplementation: isolation of new conditional-lethal mutations in each of the tubulin genes of *Saccharomyces cerevisiae*. Genetics *119*, 249–260.

Stearns, T., Hoyt, M.A., and Botstein, D. (1990). Yeast mutants sensitive to antimicrotubule drugs define three genes that affect microtubule function. Genetics *124*, 251–262.

Strathern, J.N., and Higgins, D.R. (1991). Recovery of plasmids from yeast into *Escherichia coli*: shuttle vectors. In: Guide to Yeast Genetics and Molecular Biology, vol. 194, San Diego: Harcourt Brace Jovanovich, 319–329.

Thomas, J.H., Neff, N.F., and Botstein, D. (1985). Isolation and characterization of mutations in the β-tubulin gene of *Saccharomyces cerevisiae*. Genetics *112*, 715–734.

Vale, R.D. (1991). Severing of stable microtubules by a mitotically activated protein in *Xenopus* egg extracts. Cell *64*, 827–839.

Weinstein, B., and Solomon, F. (1990). Phenotypic consequences of tubulin overproduction in *Saccharomyces cerevisiae*: differences between α-tubulin and β-tubulin. Mol. Cell. Biol. *10*, 5295–5304.

Wendell, K.L., Wilson, L., and Jordon, M.A. (1993). Mitotic block in HeLa cells by vinblastine: ultrastructural changes in kinetochore-microtubule attachment and in centrosomes. J. Cell Sci. *104*, 261–274.

Wertman, K.F., Drubin, D.G., and Botstein, D. (1992). Systematic mutational analysis of the yeast *ACT1* gene. Genetics *132*, 337–350.